Hindawi
International Journal of Energy Research
Volume 2023, Article ID 9920670, 20 pages
https://doi.org/10.1155/2023/9920670

Research Article

Energy and Exergy Assessments of a Diesel-, Biodiesel-, and Ammonia-Fueled Compression Ignition Engine

Mateusz Proniewicz,[1] **Karolina Petela**,[1] **Andrzej Szlęk**,[1] **Grzegorz Przybyła**,[1] **Ebrahim Nadimi**,[1] **Łukasz Ziółkowski**,[1] **Terese Løvås**,[2] **and Wojciech Adamczyk**[1]

[1]*Department of Thermal Technology, Silesian University of Technology, Gliwice, Poland*
[2]*Department of Energy and Process Engineering, Norwegian University of Science and Technology (NTNU), Trondheim, Norway*

Correspondence should be addressed to Mateusz Proniewicz; mproniewicz@polsl.pl

Received 20 April 2023; Revised 27 June 2023; Accepted 7 July 2023; Published 14 August 2023

Academic Editor: Amin Paykani

The research is aimed at investigating ammonia in a compression ignition internal combustion engine as a promising alternative fuel towards decarbonization. This study presents energy and exergy assessments of a low-power engine for three cases of fuel supply, diesel oil, biodiesel oil, and ammonia with pilot biodiesel oil, across the entire engine's range. While diesel or biodiesel was administered directly into the engine cylinder, the ammonia was delivered through port injection. The results show that the maximum thermal efficiency of 33.56% and exergy efficiency of 31.88% were found at 1800 rpm and 71% load for the diesel fuel system. For the biodiesel fuel system, the efficiencies were 32.72% and 30.93%, respectively, at 1800 rpm and 100% load, and for the ammonia with pilot biodiesel system, they were at 31.98% and 30.04%, respectively, for the same rpm and load. The exergy assessment indicates that exergy destruction, which accounts for the irreversibility of processes such as combustion and friction, is responsible for the greatest loss of useful energy. Optimizing these processes could significantly improve the engine's performance for all three fuel cases. This research found that ammonia could successfully substitute diesel or biodiesel fuel, as the engine's efficiency was comparable in all three tested scenarios; however, further research and optimization in terms of the ammonia-fueled engine emissions are required.

1. Introduction

Reliability, durance, and high compressive resistance have made a diesel engine a preferred application in heavy-duty vehicles, commonly used in transportation, construction, agriculture, and other sectors. However, due to the negative effect of the use of fossil fuels on climate change, there is a need to develop alternative sources of energy to decrease the emissions of greenhouse gases. This conclusion has been summarized during the 2015 Paris Agreement, resulting in the aim of the European Union of at least 55% of greenhouse gas reduction by 2030 compared to 1990 (updated in December 2020). One option to substitute fossil diesel fuel is to use a biodiesel. Technically, biodiesel consists of a mono-alkyl ester of fatty acids, produced from animal fats or plant oils (feedstock) in a transesterification process [1]. There are two main advantages of this fuel from an environmental perspective. Firstly, it is a renewable source since it is produced from resources that are continuously replenished. Secondly, it is considered carbon-neutral because the plants used for a feedstock absorb carbon dioxide during growth, thereby offsetting the CO_2 emissions that occur due to the production and combustion of the fuel [1]. In the case of a lipid feedstock, defined as waste cooking oil or animal fats/tallow and grease, the life-cycle emissions are low since the feedstock has been produced in a nonrelated process [2]. Still, there are several drawbacks associated with biodiesel. Biofuel crops compete with plants that could be otherwise used for food production, in terms of land, material, and energy consumption. This competition could result in a negative impact of the biodiesel on the environment in terms of its life cycle, considering other environmental categories than CO_2 emissions, such as land use change. There have been clearance cases of natural vegetation and forests to

grow soybeans or palm oil trees [2]. Another disadvantage in terms of its wide commercialization is the high cost of the biodiesel compared to diesel, ranging from 70% to 130% higher, as noted by the European Federation for Transport and Environment in 2022 [3]. Another option to substitute the diesel is the use an alternative like hydrogen or ammonia. Ammonia is a promising fuel due to its high energy density (caused by high hydrogen content) and a possibility of being produced from renewable sources, since it is formed from hydrogen and nitrogen, where the hydrogen can be produced via electrolysis supplied by sustainable sources. Moreover, it does not emit carbon emissions during combustion, and it can be stored and transported at moderate pressures. While sustainability is an advantage characterizing both of these fuels, hydrogen requires pressurization to approximately 700 bar or cooling to a temperature of approximately -253°C, depending on whether it is stored in gaseous or liquid form. This makes it challenging to apply broadly in the transportation sector. Easier storage, lower flammability, and a possibility to detect the ammonia by smell are some of the other advantages of ammonia over hydrogen. Furthermore, it is widely used as a fertilizer (80% of ammonia production [4]), and therefore, it already has the established infrastructure for its handling. The use of ammonia in the internal combustion engine (ICE) is limited by the parameters that make it difficult to operate: high resistance to autoignition, low flame speed, and corrosivity. As such, currently, most research is focused on implementing ammonia in spark ignition engines [5]. Yet another option in terms of substituting diesel would be electrification; however, it does not apply well to heavy vehicles that require high power output along with an acceptable range of distance. One way to assess the feasibility of utilizing an alternative fuel in the internal combustion engine is to perform an energy assessment that is based on the first law of thermodynamics. It quantifies the energy flows within the system boundaries and, therefore, allows for the estimation of energy conversion and identification of losses occurring during the operation of the engine. However, it is the second law of thermodynamics that allows for a deeper understanding of system performance, performed by assessing the quality of respective flows by means of exergy. Exergy is defined as the useful work potential considering the reference state, otherwise called as availability [6]. Exergy assessment indicates the processes in which energy is degraded, thus revealing the lost opportunities to perform work. Energy and exergy analyses are both useful tools towards the assessment of engine performance as they provide the information regarding the engine's performance and sources of energy losses and indicate which processes could be improved.

In recent years, a lot of research has been dedicated to the analysis of internal combustion engines (ICE) utilizing various fuel mixtures like diesel oil, biodiesel, methanol, hydrogen, ammonia, or mixtures of these fuels, in terms of the performance of the engine, emissions, and combustion analysis. Damanik et al. [7] presented a review of diesel engine performance and exhaust emission characteristics for diesel with biodiesel blends. They discussed the promising option of utilizing biodiesel blends with nanoadditives that decrease the carbon monoxide, nitrogen oxide, and unburned hydrocarbon emissions, while increasing the engine thermal efficiency, emphasizing that specific results depend on the biodiesel properties. Abedin et al. [8] presented a review paper on the energy balance of internal combustion engines presenting two approaches to the energy balance and discussing the case studies of alternative fuels. In a further study, Abedin et al. [9] analyzed three methods of introducing biodiesel to the engine, i.e., blend, fumigation, and emulsion, in terms of the engine performance and emissions. Thermal efficiency decreased for blend and fumigation strategies but grew in the emulsion mode. Carbon monoxide and hydrocarbon emissions increased for fumigation and emulsion strategies, but they declined in the case of the blend mode. Abdelrazek et al. [10] presented a numerical investigation comparing a direct injection diesel engine powered by base diesel oil and soybean biodiesel fuel under various load conditions. Findings showed that using soybean biodiesel fuel resulted in a decrease in carbon monoxide and hydrocarbon emissions and an increase in nitrogen oxides and carbon dioxide emissions, compared to base diesel. Additionally, an increase in brake-specific fuel consumption and a decrease in brake thermal efficiency were reported. Karpanai Selvan et al. [11] analyzed the performance of a set of the biodiesel-blended fuels in a diesel engine. It was revealed that the algae oil (AO10D) achieved higher efficiency at roughly similar levels of emissions, across the engine's load range. Thiyagarajan et al. [12] discussed the effect of hydrogen addition to biodiesel oil for the CI engine. The study revealed improvements in engine performance and reduced emissions, except for an increase in nitrogen oxides. Through numerical investigations, Ghazal [13] studied the impact of blending hydrogen with diesel in a CI engine and found improved performance, reduced emissions, and shortened ignition lag. Similarly, Jafarmadar [14] numerically investigated the mix of hydrogen and diesel and discovered a decrease in exergy efficiency as the hydrogen proportion increased. Lastly, Taghavifar et al. [15] showed a numerical analysis of hydrogen, DME, and diesel fuel systems in the CI engine which revealed that the hydrogen system offered the highest power and lowest indicated specific fuel consumption. Nadimi et al. [16] examined ammonia/biodiesel dual fuel combustion using the same small-sized single-cylinder compression ignition engine setup as in this study. Running the engine at 1500 rpm with fixed biodiesel and varied ammonia flows, the study found that ammonia could supply 69.4% of the input energy under stable conditions; however, high nitrogen oxide emissions along with ammonia slip were identified. In the further research, Nadimi et al. [17] analyzed the possibility of replacing diesel oil with an ammonia/diesel-operated engine, based on the experiments for 1200 rpm at full load varying the diesel-to-ammonia contribution ratio. The work showed that 84.2% of the input energy could be replaced by ammonia, while achieving lower carbon emissions; however, there were still high nitrogen oxides and ammonia emissions. Kuta et al. [18] investigated the dual-fuel CI ammonia engine emissions and an after-treatment process with $V_2O_5/SiO_2–TiO_2$ SCR, again using the same experimental setup as [16, 17],

comparing the diesel to ammonia (constant diesel mass flow with varying ammonia contributions). Implementation of the SCR unit allowed for a considerable reduction of nitrogen oxide emissions; however, still, the high emissions of ammonia remained unsolved. Zhang et al. [19] investigated the performance and emission characteristics of a two-stroke low-speed engine using an ammonia/diesel dual direct injection system. The work revealed that timing of diesel injection, which ignites the ammonia spray, not only enhances the indicated thermal efficiency by speeding up ammonia combustion but also minimizes NOx emissions.

Numerous papers regard the energy and exergy assessments of diesel, biodiesel, or a mixture of these two; however, relatively few papers consider the exergy assessment of utilizing alternative fuels, such as hydrogen or ammonia in the case of ICE. Al-Najem and Diab [20] performed an energy-exergy analysis on an eight-cylinder diesel engine obtaining ca. 35% of thermal efficiency. The authors discussed that around 50% of the energy contained in the fuel had been lost due to cooling and exhaust gases, whereas, based on the exergy assessment, 47% and 16% of energy in the exhaust gases and cooling water, respectively, could be potentially utilized. Şanli and Uludamar [21] reported the energy and exergy analyses of a fueled CI engine, comparing diesel to biodiesel oils: hazelnut (HB) and canola (CB). The analysis considered different engine speeds using a four-stroke and four-cylinder engine. For all three cases, the highest thermal and exergy efficiencies were obtained for 1800 rpm. Among the three variants, diesel proved to be the most preferred option, followed by HB and CB. Çakmak and Bilgin [22] performed the energy and exergy assessments of a single-cylinder diesel engine considering biodiesel fuel blends. The engine was tested under different engine speeds at full load conditions. The work showed that the blends positively contributed to the performance of the engine. A similar conclusion was found by Karami et al. [23] who also investigated the impact of using binary and ternary blends on a compression ignition diesel engine in terms of its performance and energy and exergy balances. The results demonstrated that the blends increased the exergy efficiency with a peak for a tomato-papaya blend (TPD) and decreased the percentage of heat loss exergy. An opposite finding was presented by Kul and Kahraman [24]. The assessment explored the use of biodiesel blends in diesel fuel, with each case including 5% bioethanol, under different engine speeds. Pure diesel was the variant to have obtained the highest performance in terms of the thermal and exergy efficiencies. Similarly, Nazzal and Al-Doury [25] also investigated the effect of the additional biodiesel blends to diesel fuel in terms of its impact on the energy and exergy performance, considering different engine speeds for a single-cylinder diesel engine. They discussed that higher speeds of engine promote higher exergy destruction and that adding corn oil blends decrease the thermal and exergetic efficiencies. Another work on this matter was performed by Khoobbakht et al. [26] who presented an energy and exergy assessment of a four-cylinder diesel engine for blended biodiesel and ethanol in diesel fuel with regard to engine load and speed. The results presented the negative impact of the blends on the engine's efficiency. Hoseinpour et al. [27] analyzed the effect of gasoline fumigation on energy and exergy balances for CI engines, comparing diesel fuel and B20 (20% of waste cooking oil biodiesel by volume) as baseline variants, with the gasoline introduced at two different ratios. The study revealed that the gasoline fumigation for the B20 fuel achieved higher exergy efficiency compared to that for the purely diesel case at high load. Wang et al. [28] analyzed the energy and exergy performance of a turbocharged, spark ignition four-cylinder engine supplied by hydrogen. Exergy analysis indicated a high potential—theoretically more than 59% of exergy efficiency, utilizing waste heat recovery. Yu et al. [29] compared the gasoline port injection (GPI) with hydrogen direct injection (HDI) to GPI with gasoline direct injection (GDI) in a spark ignition four-cylinder engine in terms of the energy and exergy analyses under lean burn conditions at different HDI fractions and air ratios. For both injection strategies, the thermal efficiency increased with the rise of hydrogen/gasoline direct injection fraction, and the thermal efficiency improvement achieved by HDI was higher on average by 0.64% than in the case of the GDI. The same conclusion applies to the exergy efficiency, thus showing the potential of alternative fuels. Sun et al. [30] compared two injection strategies: gasoline port fuel injection with gasoline direct injection (PFI with GDI) and port fuel injection with hydrogen direct injection (PFI with HDI) in terms of heat and exergy performance. They obtained that most of the total exergy is attributed to the exergy destruction and that utilizing hydrogen decreases the proportion of destruction. Table 1 presents a summary of energy and exergy efficiencies drawn from selected papers. All cases included, except the last one, pertain to a diesel engine using a direct injection strategy. The specific differences between the results in Table 1 can be attributed to variations in the engines tested and the characterization of the experiments. Despite these differences, the results illustrate the range of expected values.

In this research, we perform a detailed analysis, based on the first and second laws of thermodynamics, on a small compression ignition engine with port injection. This analysis spans different rotation speeds and shaft torques. Our primary objective is to explore the engine's performance across its entire range, comparing its default diesel oil fuel to a more environmentally friendly biodiesel and, finally, to ammonia, a promising alternative given environmental constraints. The secondary aim is to apply energy and exergy balance assessments to the internal combustion engine. This approach allows us to understand energy and exergy distributions, evaluate which fuel is used most efficiently, and identify potential areas for improvement. Achieving higher efficiency can lead to reduced fuel consumption and emissions, thus directly benefiting the environment.

2. Materials and Methods

The tests were performed on a single-cylinder engine Lifan C186F suited for a minitractor. The engine's specification is presented in Table 2. The engine was adjusted such that the gaseous ammonia was sent to the intake manifold to

Table 1: Comparison of selected literature on diesel engine energy and exergy efficiency.

Type of fuel	Operation condition	Maximum energy efficiency	Maximum exergy efficiency	Reference
Diesel	Constant load and speed	35.49%	34.33%	Al-Najem and Diab [20]
Biodiesel	Different load	26% at 100% load	—	Abdelrazek et al. [10]
Biodiesel or diesel	Different speed	38.85% at 1800 rpm for diesel	36.45% at 1800 rpm for diesel	Şanli and Uludamar [21]
Biodiesel/diesel mixture	Different load	46% at 100% load at 1500 rpm for AO10D	—	Karpanai Selvan et al. [11]
Biodiesel/diesel mixture	Different speed	40.41% at 2000 rpm for 10% blend	37.83% at 2000 rpm for 10% blend	Çakmak and Bilgin [22]
Biodiesel/diesel mixture	Different speed	32.12% at 1600 rpm for TPD blend	29.63% at 1600 rpm for TPD blend	Karami et al. [23]
Biodiesel/diesel mixture	Different speed	31.42% at 1400 rpm for pure diesel	29.38% at 1400 rpm for pure diesel	Kul and Kahraman [24]
Biodiesel/diesel mixture	Different speed	30.02% at 2500 rpm for pure diesel	28.16% at 2500 rpm for pure diesel	Nazzal and Al-Doury [25]
Biodiesel/diesel mixture	Different load/speed	36.61% at average	33.81% at average	Khoobbakht et al. [26]
Biodiesel or diesel/gasoline	Different load/speed	41.74% at 1300 rpm for pure B20 at 6.2 bar (break mean effective pressure)	38.32% at 1300 rpm for pure B20 at 6.2 bar (break mean effective pressure)	Hoseinpour et al. [27]
Ammonia/diesel	Constant load and speed	38% of indicated thermal efficiency for ammonia/ diesel fuel	—	Zhang et al. [19]
Hydrogen; implemented in a spark ignition engine via port injection	Different load/speed	35.1% at 2500 rpm at 0.8 MPa (brake mean effective pressure)	—	Wang et al. [28]

Table 2: Engine's specification.

Parameter	Value
Model, -	LIFAN
Engine type, -	CI, 4-stroke, 1-cylinder, forced air
Bore × stroke, mm × mm	86 × 70
Displacement, cm^3	418
Compression ratio, -	16.5 : 1
Intake valve opening, BTDC	14
Intake valve closing, ABDC	45
Exhaust valve opening, BBDC	50
Exhaust valve closing, ATDC	16
Start of injection, BTDC	15.5
Injection pressure, bar	200

mix with air before being sent to the cylinder. A Coriolis meter was used to measure the mass flow rate of ammonia, a turbine-type flowmeter was used to measure the mass flow rate of air, a thermocouple was used to measure the temperature of the exhaust gases, and an electric dynamometer was fitted to manage the engine's load and rotational speed. LabVIEW software and National Instruments hardware incorporated each of these characteristics. With an accuracy of 2% of the measurement range of the individual species, the FTIR Gasmet DX4000 was used to determine the composition of the exhaust gases. Next to the FTIR, an additional gas analyzer CAPELEC CAP 3201 was installed to provide verification and oxygen level with an accuracy of 3% of the measured value. The scheme of the experimental setup is presented in Figure 1. Nadimi et al. [16, 17] and Kuta et al. [18] have already presented the results from a different set of tests carried out using this experimental setup.

Fuels used for the purpose of the experiments have been purchased on the Polish market. The elementary analyses of diesel oil, biodiesel oil, and ammonia with corresponding lower heating values (LHV) are presented in Table 3.

Three tests considering three fuel supply scenarios were performed: diesel oil (D), biodiesel oil (B), and biodiesel oil with ammonia (B + A). The following considerations are applied:

(1) The points were measured once the engine was considered to achieve the steady state

(2) The reference conditions are the ambient conditions valid for the day and location of the tests (the tests were carried out in an open hall, thus using ambient air), summarized in Table 4

A set of measurements for each scenario included the following:

(1) *Applied shaft speed in rpm (revolutions per minute)*: 2700, 2400, 2100, 1800, 1500, and 1200

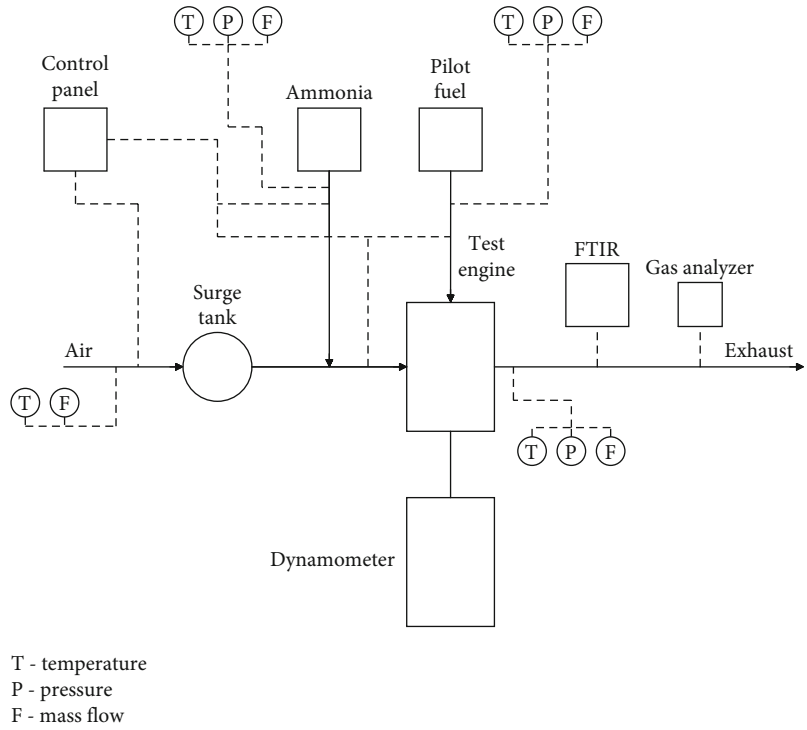

Figure 1: Diagram of experimental setup layout.

Table 3: Elementary analysis and LHV comparison of fuels.

Property	Diesel	Biodiesel	Ammonia
C, kg/kg	0.8078	0.7533	0.0000
H, kg/kg	0.1556	0.1397	0.1760
O, kg/kg	0.0363	0.1070	0.0000
N, kg/kg	0.0003	0.0000	0.8240
LHV, MJ/kg	42.4	37.4	18.6

Table 4: Ambient conditions (reference) of the three tests.

Parameter	D	B	B + A
Temperature, °C	1	3	3
Pressure, hPa	1034	1024.75	1018

(2) *Applied torque for 2700 rpm (Nm)*: 12, 8, and 4 referred to further as load in percentage (%): 100, 67, and 33

(3) *Applied torque for other speeds (Nm)*: 17, 12, 8, and 4 referred to further as load in percentage (%): 100, 71, 47, and 24

Shaft speed and torque were applied using an electric dynamometer. For a better presentation of the results, the torque range is presented in a dimensionless scale in a further part of this paper. In the case of the co-combustion of biodiesel with ammonia, the fixed mass flow rate of biodiesel was set, resulting in an applied torque of 4 Nm, and then, the increase of the torque was obtained by an increase of the ammonia mass flow rate. Such measurement design allowed for the capturing of the engine's performance throughout its operating range. The working point at 2700 rpm and 12 Nm represents the practical maximum—no higher torque was achievable when increasing the mass flow rate of ammonia. Pure diesel and biodiesel scenarios allowed for applying higher torque; however it resulted in excessive smoke emissions. Therefore, such an operating range has been considered to be practically operational.

The results of energy and exergy analyses depend on the engine's performance at respective points of operation. Therefore, a set of the most important results from the experiments is presented, as they will be supplementary for the discussion of the results. Tables 5–8 show fuel consumption; temperature of exhaust; temperature of the head of the engine; emissions of H_2O, CO_2, CO, NH_3, CH_4, and O_2; and excess air ratio. The values are presented with uncertainty defined according to equation [31]:

$$U = \sqrt{\frac{\sum \left(X_i - \bar{X}\right)^2}{n(n-1)}}, \tag{1}$$

where X_i and $\bar{X}$ stand for the measured and mean values, respectively, and n is the number of measurement results.

Excess air ratio is defined as

$$\lambda = \frac{n_a}{n_{\text{amin}}}, \tag{2}$$

where n_a is the kmol of air delivered for combustion referred

Table 5: Diesel-fueled engine-specific experiment results.

RPM, 1/min	Load	$\dot{m}_{fuel}$, g/s	T_{ex}, °C	T_{head}, °C	H_2O, %	CO_2, %	CO, %	CH_4, %	O_2, %	λ, -
2700	100%	0.322 ± 0.000	402.200 ± 0.230	71.660 ± 0.088	6.684 ± 0.008	6.548 ± 0.008	0.044 ± 0.000	0.001 ± 0.000	11.050 ± 0.331	2.36
2700	67%	0.249 ± 0.000	316.000 ± 0.111	62.910 ± 0.080	5.152 ± 0.005	5.048 ± 0.007	0.041 ± 0.000	0.001 ± 0.000	13.500 ± 0.405	3.13
2700	33%	0.180 ± 0.000	234.400 ± 0.127	53.190 ± 0.077	3.716 ± 0.005	3.485 ± 0.013	0.084 ± 0.001	0.002 ± 0.000	15.700 ± 0.471	4.42
2400	100%	0.400 ± 0.002	525.200 ± 0.050	81.300 ± 0.100	9.265 ± 0.003	9.089 ± 0.004	0.280 ± 0.002	0.002 ± 0.000	6.900 ± 0.207	1.62
2400	71%	0.276 ± 0.000	371.700 ± 0.025	68.800 ± 0.000	6.421 ± 0.008	6.336 ± 0.008	0.040 ± 0.000	0.001 ± 0.000	11.400 ± 0.342	2.41
2400	47%	0.220 ± 0.001	295.300 ± 0.075	59.150 ± 0.025	4.951 ± 0.011	4.858 ± 0.012	0.040 ± 0.000	0.001 ± 0.000	13.700 ± 0.411	3.13
2400	24%	0.163 ± 0.000	214.900 ± 0.124	46.190 ± 0.064	3.545 ± 0.006	3.327 ± 0.014	0.083 ± 0.001	0.002 ± 0.000	15.500 ± 0.465	4.16
2100	100%	0.333 ± 0.000	457.100 ± 0.193	75.380 ± 0.140	8.458 ± 0.012	8.394 ± 0.009	0.097 ± 0.001	0.002 ± 0.000	7.850 ± 0.235	1.71
2100	71%	0.243 ± 0.000	347.200 ± 0.177	72.590 ± 0.057	6.155 ± 0.012	6.066 ± 0.012	0.026 ± 0.000	0.001 ± 0.000	11.600 ± 0.348	2.38
2100	47%	0.182 ± 0.000	267.000 ± 0.172	64.800 ± 0.064	4.666 ± 0.013	4.491 ± 0.014	0.030 ± 0.000	0.001 ± 0.000	13.700 ± 0.411	3.28
2100	24%	0.133 ± 0.000	201.000 ± 0.104	56.800 ± 0.079	3.426 ± 0.004	3.123 ± 0.010	0.055 ± 0.000	0.002 ± 0.000	15.700 ± 0.471	4.58
1800	100%	0.291 ± 0.000	448.600 ± 0.140	81.150 ± 0.073	8.390 ± 0.007	8.269 ± 0.006	0.232 ± 0.001	0.004 ± 0.000	8.100 ± 0.243	1.70
1800	71%	0.204 ± 0.000	336.100 ± 0.126	76.960 ± 0.105	6.009 ± 0.005	5.894 ± 0.006	0.043 ± 0.000	0.002 ± 0.000	11.800 ± 0.354	2.44
1800	47%	0.156 ± 0.000	250.100 ± 0.157	63.990 ± 0.044	4.577 ± 0.011	4.398 ± 0.014	0.033 ± 0.000	0.002 ± 0.000	14.300 ± 0.429	3.26
1800	24%	0.111 ± 0.000	180.500 ± 0.123	55.200 ± 0.051	3.315 ± 0.008	2.919 ± 0.023	0.063 ± 0.000	0.002 ± 0.000	16.350 ± 0.490	4.65
1500	100%	0.251 ± 0.000	422.000 ± 0.188	75.240 ± 0.081	8.350 ± 0.020	8.205 ± 0.025	0.328 ± 0.004	0.008 ± 0.000	7.900 ± 0.237	1.66
1500	71%	0.178 ± 0.000	325.300 ± 0.061	76.460 ± 0.079	6.156 ± 0.003	6.053 ± 0.008	0.058 ± 0.000	0.003 ± 0.000	11.700 ± 0.351	2.36
1500	47%	0.134 ± 0.000	252.000 ± 0.238	69.430 ± 0.132	4.688 ± 0.004	4.511 ± 0.008	0.034 ± 0.000	0.003 ± 0.000	14.200 ± 0.426	3.17
1500	24%	0.094 ± 0.000	178.400 ± 0.156	59.420 ± 0.094	3.346 ± 0.010	2.992 ± 0.015	0.052 ± 0.000	0.003 ± 0.000	16.350 ± 0.490	4.62
1200	100%	0.214 ± 0.000	418.100 ± 0.398	80.960 ± 0.188	8.238 ± 0.032	8.342 ± 0.017	0.588 ± 0.010	0.018 ± 0.000	6.950 ± 0.208	1.48
1200	71%	0.152 ± 0.000	332.600 ± 0.085	79.560 ± 0.016	6.529 ± 0.006	6.471 ± 0.017	0.143 ± 0.001	0.008 ± 0.000	10.500 ± 0.315	2.08
1200	47%	0.109 ± 0.000	251.800 ± 0.165	74.510 ± 0.094	4.945 ± 0.007	4.754 ± 0.013	0.050 ± 0.000	0.005 ± 0.000	13.300 ± 0.399	2.93
1200	24%	0.078 ± 0.000	176.600 ± 0.257	61.510 ± 0.103	3.453 ± 0.011	3.207 ± 0.025	0.058 ± 0.000	0.005 ± 0.000	15.700 ± 0.471	4.35

Table 6: Biodiesel-fueled engine-specific experiment results.

RPM, 1/min	Load	$\dot{m}_{fuel}$, g/s	T_{ex}, °C	T_{head}, °C	H_2O, %	CO_2, %	CO, %	CH_4, %	O_2, %	λ, -
2700	100%	0.350 ± 0.002	415.700 ± 0.231	80.640 ± 0.129	6.658 ± 0.007	6.940 ± 0.006	0.072 ± 0.000	0.001 ± 0.000	10.600 ± 0.318	2.21
2700	67%	0.267 ± 0.000	313.600 ± 0.228	68.170 ± 0.067	4.993 ± 0.008	5.207 ± 0.015	0.042 ± 0.000	0.001 ± 0.000	13.300 ± 0.399	2.97
2700	33%	0.194 ± 0.000	234.600 ± 0.189	59.180 ± 0.071	3.522 ± 0.010	3.526 ± 0.014	0.073 ± 0.000	0.002 ± 0.000	15.600 ± 0.468	4.18
2400	100%	0.448 ± 0.000	517.900 ± 0.284	79.360 ± 0.161	9.049 ± 0.011	9.465 ± 0.016	0.349 ± 0.003	0.005 ± 0.000	9.200 ± 0.276	1.50
2400	71%	0.316 ± 0.000	384.800 ± 0.135	75.910 ± 0.079	6.390 ± 0.008	6.677 ± 0.012	0.065 ± 0.000	0.003 ± 0.000	12.900 ± 0.387	2.18
2400	47%	0.236 ± 0.000	291.600 ± 0.152	65.340 ± 0.065	4.802 ± 0.006	4.977 ± 0.018	0.043 ± 0.000	0.003 ± 0.000	13.900 ± 0.417	2.99
2400	24%	0.170 ± 0.000	214.500 ± 0.133	56.190 ± 0.039	3.431 ± 0.005	3.335 ± 0.010	0.071 ± 0.000	0.003 ± 0.000	15.800 ± 0.474	4.26
2100	100%	0.386 ± 0.000	449.400 ± 0.418	68.930 ± 0.227	8.278 ± 0.021	8.550 ± 0.017	0.176 ± 0.002	0.009 ± 0.000	9.500 ± 0.285	1.63
2100	71%	0.271 ± 0.000	341.100 ± 0.230	73.200 ± 0.079	5.899 ± 0.018	6.137 ± 0.018	0.050 ± 0.000	0.004 ± 0.000	13.700 ± 0.411	2.33
2100	47%	0.206 ± 0.000	264.500 ± 0.079	64.800 ± 0.055	4.546 ± 0.005	4.664 ± 0.005	0.039 ± 0.000	0.004 ± 0.000	15.700 ± 0.471	3.14
2100	24%	0.146 ± 0.000	193.300 ± 0.178	56.330 ± 0.052	3.286 ± 0.013	3.153 ± 0.017	0.060 ± 0.001	0.003 ± 0.000	17.900 ± 0.537	4.57
1800	100%	0.327 ± 0.000	419.800 ± 0.194	67.960 ± 0.200	7.829 ± 0.007	8.097 ± 0.027	0.293 ± 0.001	0.016 ± 0.000	9.400 ± 0.282	1.69
1800	71%	0.239 ± 0.000	326.300 ± 0.083	70.780 ± 0.047	5.795 ± 0.006	6.032 ± 0.004	0.087 ± 0.000	0.010 ± 0.000	13.100 ± 0.393	2.31
1800	47%	0.178 ± 0.000	250.200 ± 0.120	63.970 ± 0.053	4.470 ± 0.010	4.479 ± 0.027	0.054 ± 0.000	0.006 ± 0.000	15.800 ± 0.474	3.14
1800	24%	0.125 ± 0.000	178.600 ± 0.063	55.650 ± 0.048	3.188 ± 0.002	2.972 ± 0.009	0.075 ± 0.000	0.005 ± 0.000	17.800 ± 0.534	4.53
1500	100%	0.292 ± 0.000	423.200 ± 0.391	75.370 ± 0.240	8.344 ± 0.012	8.494 ± 0.018	0.476 ± 0.003	0.022 ± 0.000	8.300 ± 0.249	1.59
1500	71%	0.207 ± 0.000	327.800 ± 0.172	78.840 ± 0.088	6.004 ± 0.021	6.214 ± 0.022	0.097 ± 0.001	0.010 ± 0.000	12.500 ± 0.375	2.25
1500	47%	0.156 ± 0.000	250.200 ± 0.044	67.530 ± 0.039	4.645 ± 0.003	4.681 ± 0.012	0.058 ± 0.000	0.008 ± 0.000	14.300 ± 0.429	3.02
1500	24%	0.109 ± 0.000	179.600 ± 0.106	59.720 ± 0.064	3.331 ± 0.003	3.121 ± 0.010	0.062 ± 0.000	0.006 ± 0.000	16.200 ± 0.486	4.37
1200	100%	0.254 ± 0.002	440.800 ± 3.700	99.600 ± 0.400	8.491 ± 0.019	8.426 ± 0.045	1.368 ± 0.025	0.029 ± 0.000	7.800 ± 0.234	1.35
1200	71%	0.171 ± 0.000	324.200 ± 0.246	81.370 ± 0.052	5.910 ± 0.019	6.182 ± 0.021	0.162 ± 0.002	0.019 ± 0.000	11.600 ± 0.348	2.06
1200	47%	0.127 ± 0.000	243.600 ± 0.088	69.820 ± 0.044	4.668 ± 0.006	4.750 ± 0.014	0.084 ± 0.001	0.011 ± 0.000	14.000 ± 0.420	2.85
1200	24%	0.087 ± 0.000	165.800 ± 0.109	57.780 ± 0.035	3.301 ± 0.006	3.070 ± 0.012	0.078 ± 0.000	0.007 ± 0.000	16.300 ± 0.489	4.23

Table 7: Ammonia-fueled engine-specific experiment results.

RPM, 1/min	Load	$\dot{m}_{fuel}$, g/s	T_{ex}, °C	T_{head}, °C	H_2O, %	CO_2, %	CO, %	CH_4, %	O_2, %	λ, -
2700	100%	0.201 ± 0.000	387.100 ± 0.046	63.900 ± 0.033	11.700 ± 0.030	4.527 ± 0.033	0.067 ± 0.000	0.005 ± 0.000	10.200 ± 0.306	3.63
2700	67%	0.203 ± 0.000	310.400 ± 0.034	56.820 ± 0.019	7.527 ± 0.007	4.798 ± 0.021	0.093 ± 0.000	0.006 ± 0.000	12.900 ± 0.387	3.71
2700	33%	0.194 ± 0.000	234.600 ± 0.189	59.180 ± 0.071	3.522 ± 0.010	3.526 ± 0.014	0.073 ± 0.000	0.002 ± 0.000	15.600 ± 0.468	4.10
2400	100%	0.184 ± 0.000	446.200 ± 0.108	73.660 ± 0.049	15.860 ± 0.013	4.652 ± 0.027	0.085 ± 0.000	0.006 ± 0.000	9.000 ± 0.270	3.31
2400	71%	0.181 ± 0.000	360.900 ± 0.073	62.950 ± 0.071	10.620 ± 0.009	4.402 ± 0.060	0.057 ± 0.000	0.006 ± 0.000	10.500 ± 0.315	3.59
2400	47%	0.180 ± 0.000	284.900 ± 0.023	56.650 ± 0.021	7.139 ± 0.004	4.466 ± 0.022	0.075 ± 0.000	0.006 ± 0.000	13.300 ± 0.399	3.88
2400	24%	0.170 ± 0.000	214.500 ± 0.133	56.190 ± 0.039	3.431 ± 0.005	3.335 ± 0.010	0.071 ± 0.000	0.003 ± 0.000	15.800 ± 0.474	4.26
2100	100%	0.153 ± 0.001	422.900 ± 0.150	77.710 ± 0.069	16.280 ± 0.030	3.852 ± 0.026	0.078 ± 0.001	0.006 ± 0.000	6.900 ± 0.207	3.62
2100	71%	0.155 ± 0.000	326.900 ± 0.147	63.360 ± 0.084	10.080 ± 0.008	3.802 ± 0.054	0.040 ± 0.000	0.007 ± 0.000	11.100 ± 0.333	3.85
2100	47%	0.155 ± 0.000	260.300 ± 0.024	57.540 ± 0.029	6.849 ± 0.004	3.929 ± 0.013	0.056 ± 0.000	0.008 ± 0.000	13.700 ± 0.411	4.09
2100	24%	0.146 ± 0.000	193.300 ± 0.178	56.330 ± 0.052	3.286 ± 0.013	3.153 ± 0.017	0.060 ± 0.001	0.003 ± 0.000	17.900 ± 0.537	4.57
1800	100%	0.129 ± 0.000	391.000 ± 0.223	74.360 ± 0.083	15.950 ± 0.040	3.180 ± 0.049	0.090 ± 0.001	0.024 ± 0.000	7.000 ± 0.210	3.80
1800	71%	0.128 ± 0.000	303.100 ± 0.078	62.030 ± 0.065	10.050 ± 0.108	3.001 ± 0.028	0.052 ± 0.000	0.019 ± 0.000	11.500 ± 0.345	4.12
1800	47%	0.131 ± 0.000	244.400 ± 0.112	58.170 ± 0.009	6.638 ± 0.016	3.732 ± 0.014	0.066 ± 0.000	0.016 ± 0.000	14.000 ± 0.420	4.19
1800	24%	0.125 ± 0.000	178.600 ± 0.063	55.650 ± 0.048	3.188 ± 0.002	2.972 ± 0.009	0.075 ± 0.000	0.005 ± 0.000	17.800 ± 0.534	4.53
1500	100%	0.111 ± 0.000	372.000 ± 0.147	75.870 ± 0.095	16.200 ± 0.054	3.393 ± 0.041	0.133 ± 0.001	0.030 ± 0.000	7.250 ± 0.217	3.46
1500	71%	0.110 ± 0.000	291.500 ± 0.102	62.800 ± 0.078	10.440 ± 0.061	3.170 ± 0.031	0.070 ± 0.000	0.020 ± 0.000	11.950 ± 0.358	3.34
1500	47%	0.111 ± 0.000	234.900 ± 0.136	58.350 ± 0.018	6.790 ± 0.026	3.658 ± 0.015	0.071 ± 0.000	0.014 ± 0.000	14.600 ± 0.438	3.38
1500	24%	0.109 ± 0.000	179.600 ± 0.106	59.720 ± 0.064	3.331 ± 0.004	3.121 ± 0.011	0.062 ± 0.000	0.006 ± 0.000	16.200 ± 0.486	4.39
1200	100%	0.093 ± 0.000	353.000 ± 0.071	77.390 ± 0.108	16.450 ± 0.068	3.606 ± 0.033	0.175 ± 0.002	0.036 ± 0.000	7.500 ± 0.225	3.31
1200	71%	0.092 ± 0.000	279.800 ± 0.125	63.580 ± 0.090	10.840 ± 0.013	3.338 ± 0.034	0.088 ± 0.000	0.021 ± 0.000	12.400 ± 0.372	3.64
1200	47%	0.090 ± 0.000	225.400 ± 0.161	58.520 ± 0.027	6.941 ± 0.036	3.584 ± 0.015	0.076 ± 0.000	0.013 ± 0.000	15.200 ± 0.456	3.96
1200	24%	0.087 ± 0.000	165.800 ± 0.109	57.780 ± 0.035	3.301 ± 0.006	3.070 ± 0.012	0.078 ± 0.000	0.007 ± 0.000	16.300 ± 0.489	4.23

Table 8: Ammonia-fueled engine: ammonia consumption and emission in the exhaust experiment results.

RPM, 1/min	Load	Ammonia consumption, kg/h	NH_3, %
2700	100%	1.481 ± 0.000	1.468 ± 0.003
2700	67%	0.835 ± 0.000	1.047 ± 0.004
2700	33%	0.000 ± 0.000	0.000 ± 0.000
2400	100%	1.770 ± 0.000	1.540 ± 0.002
2400	71%	1.246 ± 0.000	1.439 ± 0.005
2400	47%	0.631 ± 0.000	0.879 ± 0.001
2400	24%	0.000 ± 0.000	0.000 ± 0.000
2100	100%	1.726 ± 0.000	1.627 ± 0.005
2100	71%	1.140 ± 0.000	1.476 ± 0.002
2100	47%	0.608 ± 0.000	0.916 ± 0.002
2100	24%	0.000 ± 0.000	0.000 ± 0.000
1800	100%	1.542 ± 0.000	1.625 ± 0.004
1800	71%	1.011 ± 0.000	1.452 ± 0.002
1800	47%	0.511 ± 0.000	0.911 ± 0.002
1800	24%	0.000 ± 0.000	0.000 ± 0.000
1500	100%	1.282 ± 0.000	1.576 ± 0.004
1500	71%	0.852 ± 0.000	1.463 ± 0.005
1500	47%	0.444 ± 0.000	0.947 ± 0.003
1500	24%	0.000 ± 0.000	0.000 ± 0.000
1200	100%	1.022 ± 0.000	1.528 ± 0.004
1200	71%	0.693 ± 0.000	1.473 ± 0.007
1200	47%	0.378 ± 0.000	0.984 ± 0.003
1200	24%	0.000 ± 0.000	0.000 ± 0.000

per kg of fuel and n_{amin} is the stoichiometric amount of air required to combust the fuel. In the case of the experimental results of the ammonia-fueled engine, seen in Table 7, the excess air ratio is referred per the amount of pilot fuel (biodiesel).

The values, along with their associated uncertainties, were calculated on a dataset that had been progressively fragmented over time and refined by the removal of outlier points. The objective was to conduct the measurement as soon as the engine reached a steady-state condition. Hence, all measured values were continuously logged, and once there was no significant variance between subsequent measurements, the data for a specific operating point was recorded. This was followed by a data-cleaning process, which resulted in a final set of measured values that were closely aligned. When equation (19) was applied to such closely clustered measurement values, the resulting uncertainty was very small. The exception is O_2 that was measured by an additional gas analyzer, and therefore, it uses a fixed value of uncertainty. The uncertainties for exhaust components like CO, CH_4, and NH_3 are essentially zero, since they were measured in ppm, whereas the presented values regard the percentage shares. The emissions are not referred per 5% of O_2 share, which is required for the comparison of the emissions from different engines and is a common literature approach, e.g., [16], but they are shown directly in a form they are used for energy and exergy balances.

From the experimental results reported in Tables 5 and 6, it is evident that high loads and speed of the shaft require high fuel consumption, thus promoting higher temperatures of both exhaust and engine's head which is true at all shaft speeds for all three cases. The excess air ratio decreases along with the increase in the load, and it achieves similar values to the corresponding loads, independently of the rpm. A low excess air ratio corresponds to high H_2O, CO_2, CO, and CH_4 at low O_2, and these proportions reverse with an increase of the excess air ratio. On average, the ammonia-fueled scenario, presented in Tables 7 and 8, achieves a lower temperature of exhaust and engine's head. Since the carbon emissions for this case originate from a pilot dosage equivalent to 4 Nm of applied torque, as explained in Section 2, such a solution allows for the reduction of CO_2 and CH_4 emissions. A high load promotes high H_2O and NH_3 shares due to high ammonia consumption and ammonia slip; CO_2, CO, and CH_4 take roughly similar values for 100%, 71%, and 47% loads at any given rpm.

3. Energy and Exergy Analysis Approach

The mass and energy balances of the control volume in a steady-state condition can be written consecutively as

$$\sum \dot{m}_{in} = \sum \dot{m}_{out}, \tag{3}$$

$$\sum \dot{m} h_{in} = \sum \dot{m} h_{out}, \tag{4}$$

where the subscripts "in" and "out" stand for the inlet and outlet, respectively; $\dot{m}$ refers to the mass flow rate; and h refers to the specific enthalpy.

The energy balance can be rewritten as

$$\dot{Q}_{air} + \dot{E}_{fuel} = \dot{W} + \dot{Q}_{lost} + \dot{Q}_{exh}, \tag{5}$$

where $\dot{Q}$ with subscript "air" stands for the energy rate delivered by air, $\dot{E}$ with subscript "fuel" stands for the fuel energy rate, $\dot{W}$ stands for the power of the engine, $\dot{Q}$ with subscript "lost" stands for net heat transfer rate lost to the environment (later also noted as cooling losses), and $\dot{Q}$ with subscript "exh" stands for the energy rate of the exhaust gases equal to the physical enthalpy of the exhaust gases.

Considering the intake air to be at the same temperature as the reference conditions, the physical enthalpy of air entering the control volume can be neglected; the same consideration applies to the physical enthalpy of fuel. Potential and kinetic energies of fluid streams are omitted.

Fuel energy rate can be expressed as

$$\dot{E}_{fuel} = \dot{m}_{fuel} LHV_{fuel}, \tag{6}$$

where $\dot{m}$ with subscript "fuel" stands for the mass flow rate of fuel and LHV with subscript "fuel" indicates the lower heating value of the fuel.

Enthalpy of exhaust gases is expressed as

$$\dot{Q}_{\text{exh}} = \sum \dot{m}_{\text{exh},i} \Delta h_{\text{exh},i}, \tag{7}$$

where $\dot{m}$ with subscript "exh,i" stands for the mass flow rate of the i component of exhaust gases and Δh with subscript "exh,i" represents the difference of specific enthalpy of the i component of exhaust gases at the measured and reference state temperatures, and it is defined as

$$\Delta h_i = h_i - h_{i,0}. \tag{8}$$

Heat transfer rate lost to the environment is calculated by closing the energy balance. Thermal efficiency of the engine is calculated as

$$\eta = \frac{\dot{W}}{\dot{E}_{\text{fuel}}}. \tag{9}$$

Based on the defined energy balance, the exergy balance of the control volume equals to the following:

$$\dot{\text{E}}\text{x}_{\text{fuel}} = \dot{\text{E}}\text{x}_{\text{w}} + \dot{\text{E}}\text{x}_{\text{lost}} + \dot{\text{E}}\text{x}_{\text{exh}} + \dot{\text{E}}\text{x}_{\text{dest}}, \tag{10}$$

where Ėx with subscript "fuel" indicates the exergy fuel rate, Ėx with subscript "w" stands for the exergy work rate, Ėx with subscript "lost" means the exergy rate lost to the environment, Ėx with subscript "exh" stands for the exergy of exhaust gases, and Ėx with subscript "dest" represents the exergy destruction rate.

Th exergy fuel rate is defined as

$$\dot{\text{E}}\text{x}_{\text{fuel}} = \dot{m}_{\text{fuel}} \varepsilon_{\text{ch,fuel}}, \tag{11}$$

where $\varepsilon_{\text{ch,fuel}}$ stands for the specific chemical exergy of fuel.

For liquid fuels, the standard chemical exergy of fuel can be calculated based on its elemental analysis. There are several approaches proposed in the literature, as summarized by Michalakakis et al. [32]. In this work, the equation proposed by Szargut is used [33] to determine the chemical exergy of diesel and biodiesel:

$$\varepsilon_{\text{ch,fuel}} = \text{LHV}_{\text{fuel}} \left[1.047 + 0.0154 \frac{\text{H}}{\text{C}} + 0.0562 \frac{\text{O}}{\text{C}} + 0.5904 \frac{\text{N}}{\text{C}} \left(1 - 0.175 \frac{H}{C} \right) \right], \tag{12}$$

where H, C, O, and N represent the mass fractions of hydrogen, carbon, oxygen, and nitrogen, respectively, from the ultimate analysis of the fuel sample.

The standard chemical exergy of ammonia is taken directly from the literature (Szargut [34]), and it is equal to 337.9 kJ/mol.

The exergy work rate is equal to the net work of the engine:

$$\dot{\text{E}}\text{x}_{\text{w}} = \dot{W}. \tag{13}$$

Table 9: Ambient environment (reference) definition.

Component	Mol fraction, %
yCO	7.00E-04
$y\text{CO}_2$	3.45E-02
$y\text{H}_2\text{O}$	3.03
$y\text{N}_2$	75.67
$y\text{O}_2$	20.35
$y\text{NH}_3$	6.00E-07
$y\text{CH}_4$	1.74E-04
Rest	9.15E-01

The exergy rate lost to the environment equals to

$$\dot{\text{E}}\text{x}_{\text{lost}} = \sum \left(1 - \frac{T_0}{T_m} \right) \dot{Q}_{\text{lost}}, \tag{14}$$

where T with subscript "0" is the temperature at the reference state and T with subscript "m" stands for the temperature of the system boundary where heat is transferred to the environment, as explained in [35]. Most analyses found in the literature used for the experiment the water-cooled engine, and therefore, the temperature of cooling water is used as this temperature, e.g., [24, 26]; however, since the engine used in the experiment is cooled by air, the temperature of the head of the engine is here considered.

The exergy of exhaust gases can be written as

$$\dot{\text{E}}\text{x}_{\text{exh}} = \sum \dot{m}_{\text{exh},i} \varepsilon_{\text{exh},i}, \tag{15}$$

where ε with subscript "exh,i" is the specific exergy of the i exhaust component defined as

$$\varepsilon_{\text{exh}} = \varepsilon_{\text{tm}} + \varepsilon_{\text{ch}}, \tag{16}$$

where ε with the subscript "tm" represents the specific thermomechanical exergy defined as

$$\varepsilon_{\text{tm}} = \Delta h - T_0 \Delta s, \tag{17}$$

where s stands for the specific entropy.

Specific chemical exergy of the exhaust gases is calculated according to the following formula:

$$\varepsilon_{\text{ch}} = \dot{R} T_0 \ln \frac{y_i}{y_{i,r}}, \tag{18}$$

where $\dot{R}$ is the universal gas constant equal to 8.314 J·mol^{-1}·K^{-1}, y_i is the molar fraction of the i component in the exhaust gases, and $y_{i,r}$ stands for the molar fraction of the i component in a reference environment.

The molar fractions of the components present in the environment are shown in Table 9. The assumption of ideal gases applies.

The components listed in Table 9 are taken from the following sources:

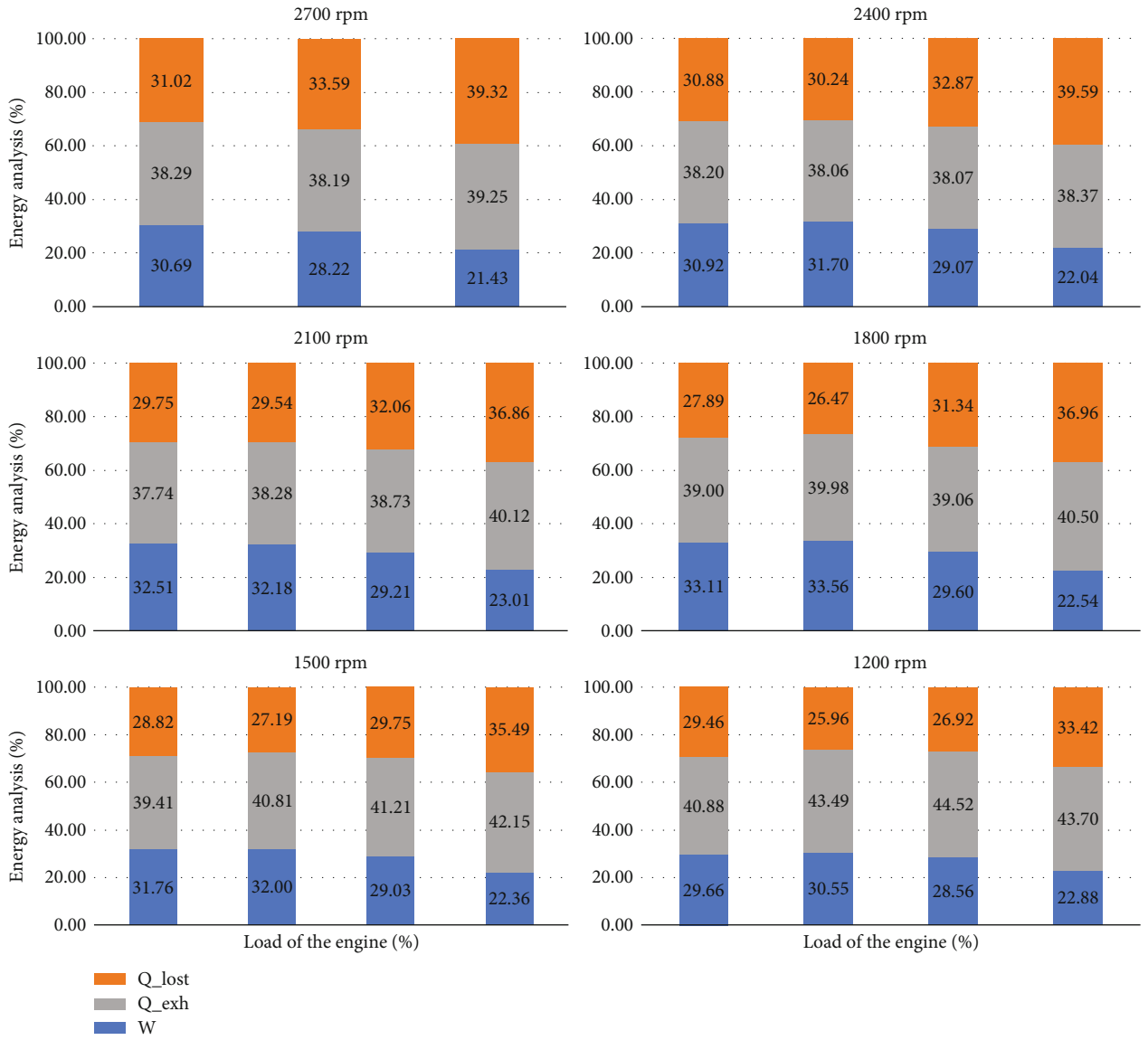

Figure 2: Results of energy analysis of diesel-fueled engine.

(1) Concentrations of CO, CO_2, H_2O, N_2, and O_2 follow the literature approach [21, 26]

(2) The concentration of NH_3 is considered to be 6 ppb (averaged global value of atmospheric NH_3 based on a satellite remote measurement), assumed from the review paper [36]

(3) The concentration of CH_4 is assumed from [37] (recalculated from the dry air composition)

It is common in the literature that the concentrations of NH_3 or CH_4 are not included in the energy and exergy balances (e.g., [21, 24, 26]); however, this paper is aimed at a detailed investigation of chemical exergy losses in the exhaust part, especially due to a high share of ammonia in the exhaust for the co-combustion of biodiesel with ammonia, as seen in Tables 7 and 8.

The exergy destruction rate is calculated from closing the exergy balance. It represents the rate of energy accounted in the irreversible processes such as combustion and friction.

Exergy efficiency is defined as

$$\psi = \frac{\dot{E}x_w}{\dot{E}x_{fuel}}. \tag{19}$$

4. Results

4.1. Diesel-Fueled Engine. Results of energy analysis applied on the measured data concerning the shaft's speeds and applied loads are presented in Figure 2. Thermal efficiency, a measure of how effectively an engine transforms the energy from the fuel into the useful work, is impacted by several factors that influence engine performance. These include exhaust losses, cooling efficiency, combustion effectiveness,

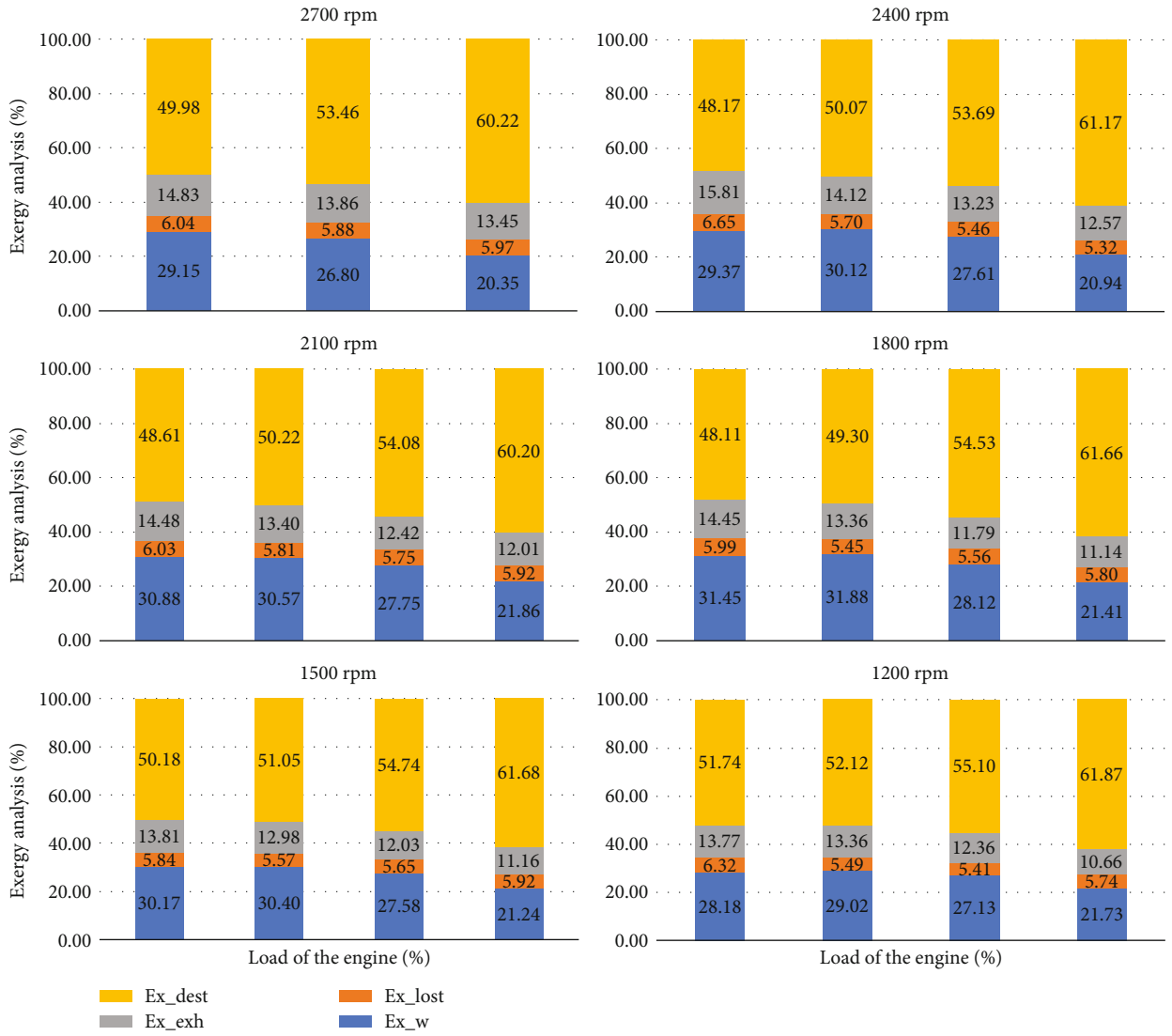

Figure 3: Results of exergy analysis of diesel-fueled engine.

and friction within the engine. Noting the case of 2400 rpm in Figure 2, these dependencies could be described in the following way. At 100% load and 2400 rpm, the engine achieves 30.92% of thermal efficiency which is due to the high temperature of exhaust gases at an excess air ratio of ca. 1.62. Peak efficiency of 31.70% for 2400 rpm is obtained at 71% load, at a lower temperature of the head of the engine resulting in a slight decrease in cooling losses and a lower exhaust temperature, even though the mass flow rate of the exhaust is higher (excess air ratio of 2.41, as presented in the Table 5). As a result, there is a slightly lower share of exhaust energy (analyzing the exergy efficiency for this point in Figure 3, it is seen that even though at 71% the exergy destruction associated with combustion is higher, lower shares of exhaust exergy and exergy lost to the environment result in an improvement in terms of the engine efficiency). Along with the decline in the load, the lower efficiencies are seen which are due to an increase in the ratio between friction losses and the engine-indicated work [17] (confirmed by the increased share of exergy destruction rate, seen in Figure 3) and high exhaust energy share caused by the higher exhaust mass flow rates (high excess air ratios of 3.13 and 4.16, as seen in Table 5, respectively, at 47% and 24% loads).

Collating it to the results at other rpm, the general trend is that the efficiencies take similar values at corresponding loads (e.g., for a load of 47%: efficiency is 29.21% at 2100 rpm and 29.03% and 1500 rpm), independently of the shaft's speed. In the case of 2700 rpm, the 100% load corresponds to 12 Nm of applied torque, and therefore, the behavior for 2700 rpm mirrors the trend of other rpm between the 71% load and 24% load, and so, the 100% load at 2700 rpm would be around the peak efficiency for this rpm. Noting the case of 2100 rpm, the highest efficiency is obtained at 100% load, not 71% as for other shaft speeds; however, the difference between the efficiencies for these two points is ca. 0.3 percentage point. At 71% load, there is a higher excess air ratio; however, a lower exhaust temperature compensates for the value of the exhaust energy, so that it is very similar at both of these points. The lower temperature of the

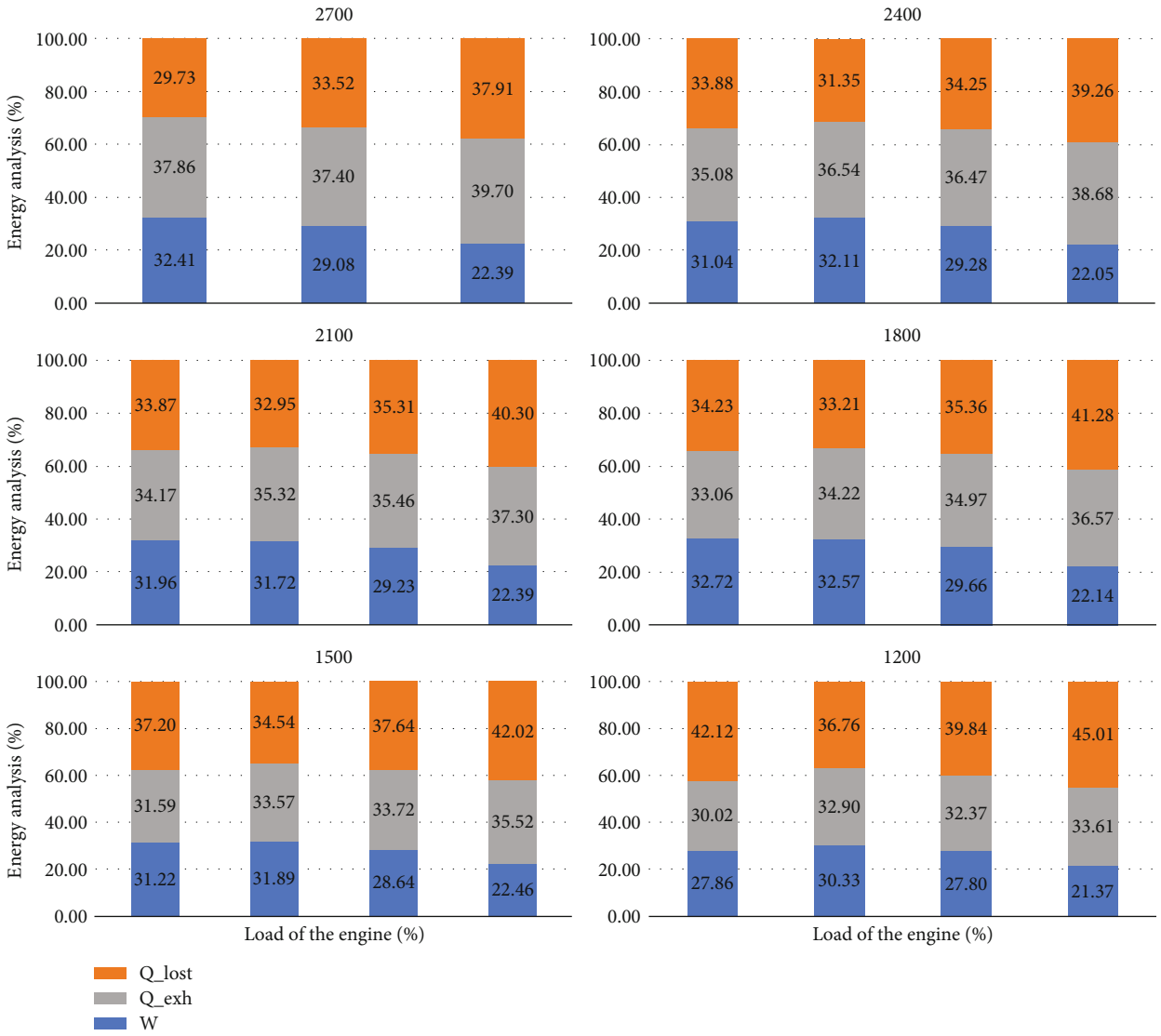

Figure 4: Results of energy analysis of biodiesel-fueled engine.

engine's head is registered at 71% load; however, since the 100% load is characterized by the lowest exergy destruction losses (accounting for combustion and friction; seen in Figure 3), a slightly higher efficiency is achieved at this point. Considering the thermal efficiency to be the main criterion of the engine's performance, the optimized operation of the diesel-fueled engine would be at medium-high loads, preferably between 1500 and 2400 rpm. Across the engine's working range, the peak efficiency of 33.56% is achieved at 1800 rpm with a load of 71%.

Applying exergy balance leads to the same conclusion. Based on Figure 3, it is seen that exergy efficiency follows the energy efficiency trend; however, it takes lower values, since it is defined based on the exergy fuel input. The peak exergy efficiency across the engine's operating range is achieved for the same point as in the case of energy efficiency (1800 rpm and 71% load) with the value of 31.88%. Noting the case of 2400 rpm, it is seen that it is the combustion process along with friction that is responsible for most of the energy degradation, seen by the highest share of exergy destruction at all loads. Exergy destruction increases along with the decrease in load; it is the highest at the 24% load at each rpm. The exergy of heat lost to the environment decreases with a decline in load which is caused by the lower temperature of the engine's head. In this work, the temperature of the engine head serves as a reference for determining the exergy rate lost to the environment; however, if the engine was cooled by the water and the temperature of cooling water would be used, which is the most common approach, e.g., [24, 26], it would decrease the share of exergy lost to the cooling by a few percentage points and increase the share of exergy destruction, thus not impacting the conclusions. The trend regarding the exergy of the exhaust is that a high temperature of exhaust gases, which occurs at high load, increases the share of exhaust exergy. It is seen that, independently from the rpm and load, for all cases, this value reaches above 10% in reference to the fuel exergy input.

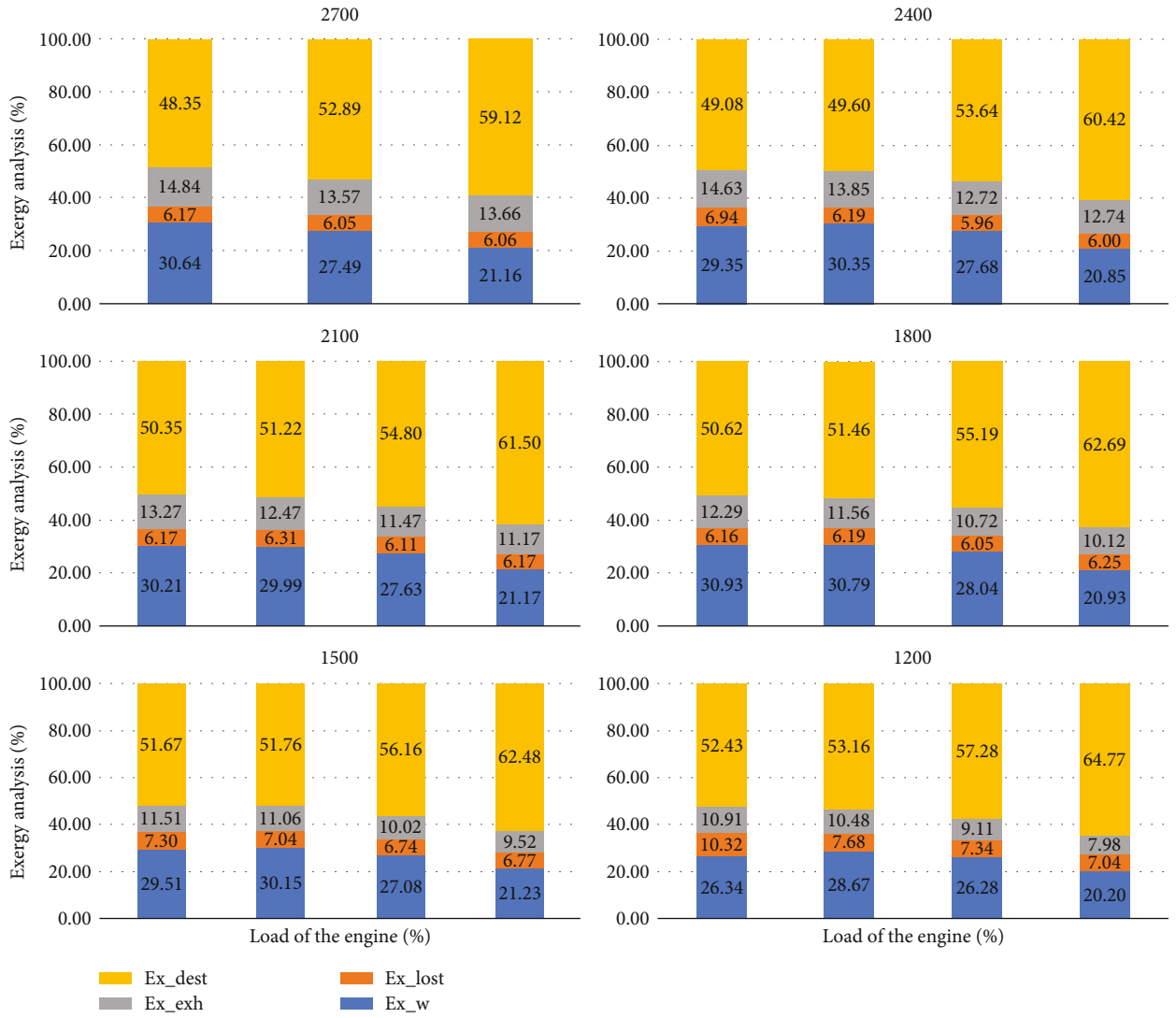

Figure 5: Results of exergy analysis of biodiesel-fueled engine.

Assuming a modification to the engine that would allow for a waste heat recovery system to transform all of the exhaust exergy into work, an efficiency of 45.90% could be found at 1800 rpm and a 100% load. However, from the second law of thermodynamics, it is known that such heat transfer cannot occur without any losses; therefore, such efficiency should be treated as a theoretical concept. The design of a waste heat recovery system aiming to recover as much exhaust exergy as possible depends on a variety of factors. These include the size and weight of the system, its cost, complexity, and the balance between efficiency gains and the operating conditions of the vehicle.

4.2. Biodiesel-Fueled Engine. The results of energy and exergy assessments for the biodiesel-fueled engine are presented in Figures 4 and 5. Noting the case of 2400 rpm, it is seen that the trends regarding the energy and exergy distributions remain similar to the case of the diesel-fueled scenario, and therefore, further description will aim at capturing the crucial differences. The peak efficiency occurs at 100% load at 2700, 2100, and 1800 rpm (for the diesel case, this is true only for 2700 and 2100 rpm); for other speeds, it occurs at 71% load. The reason for this trend is addressed in the previous Section 4.1; the explanation of this is best seen in Figure 5. For 2700, 2100, and 1800 rpm, the effect of lower exhaust exergy and exergy lost to the environment for the 71% load prevails at the lowest combustion losses at 100%; for the other speeds, it is the opposite. The overall highest thermal efficiency across the entire engine's range is 32.72%, for 1800 rpm and 100% load. This value is very close to the efficiency obtained at the same rpm but with a 71% load. Moreover, it is also near the efficiency achieved at a higher rpm of 2700, still at 100% load. The difference among these three efficiency values is less than one percentage point. The overall highest exergy efficiency is achieved at 1800 rpm and 100% load with the value of 30.93%, following the thermal efficiency trend.

Compared to the diesel case, for 2400 rpm and lower shaft speeds, the share of exhaust energy is a few percentage points lower (at all loads; at 2700 rpm, the differences are

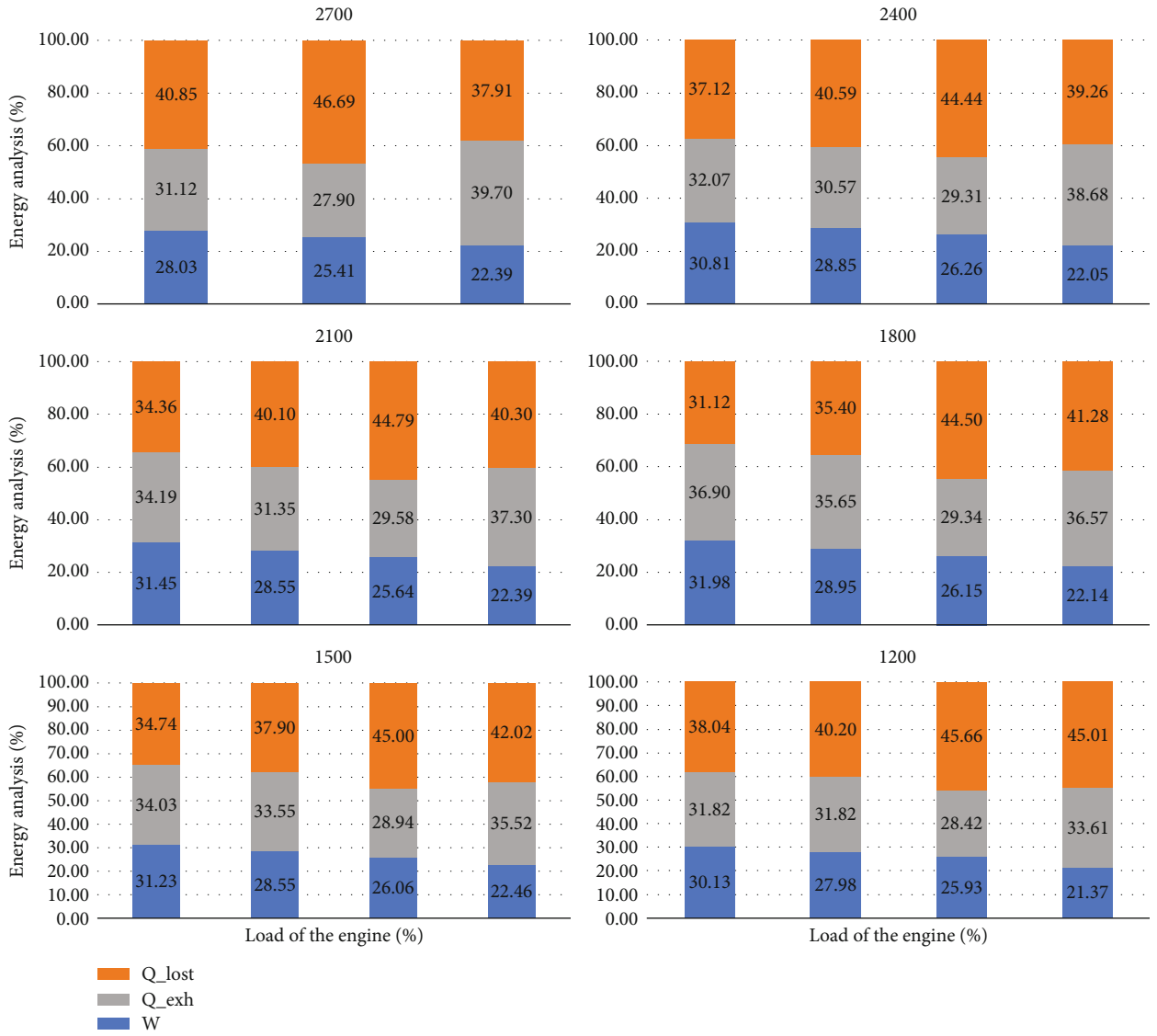

Figure 6: Results of energy analysis of ammonia-fueled engine.

even smaller). It is caused by the difference in the combustion process since a biodiesel-fueled engine is characterized by a higher fuel consumption due to its lower value of LHV, but lower excess air ratio, resulting in an overall lower mass flow rate of the exhaust. Shares of carbon monoxide and oxygen in the exhaust are higher indicating less complete combustion, as seen in Tables 5 and 6. This observation is confirmed by the exergy analysis which shows that the share of exergy destruction is higher for the biodiesel case (seen for 2400 rpm and lower rpm values, independently of loads). For 2700 rpm, it is actually the opposite, where the biodiesel case achieves slightly higher efficiency at all loads due to lower exergy destruction losses, noting the exhaust and cooling exergies to be similar. Theoretically, the maximum efficiency, given the waste heat recovery allowing for full utilization of the exhaust, would be the 45.48% at 2700 rpm and a 100% load.

4.3. Ammonia-Fueled Engine. Figures 6 and 7 present the results of energy and exergy analyses for the co-combustion of an ammonia-fueled engine. Noting that the biodiesel mass flow rate was set as a fixed value resulting in 4 Nm of applied torque, the results for the 24% load are the same as those in Figures 4 and 5. Focusing on Figures 6 and 7, independently of the shaft's speeds, the following trends can be observed. Low loads promote lower exhaust energy and an increase in the cooling, coupled with the decrease in thermal efficiency. A decreasing effect of the exhaust energy along with the decline in the torque is caused by a dominating effect of a declining temperature of the exhaust, even though there is an increase in the mass flow rate of the exhaust. In the case of the diesel and biodiesel variant, the differences between the exhaust energies at respective loads are smaller than in the case of the ammonia-fueled engine. Exergy destruction, accounting for the combustion and friction processes, increases with decline of the load which is the general trend. Exhaust exergy takes the highest value at the maximum load and gradually decreases (since it is related to the exhaust temperature). Decreasing the load also causes the decline in the

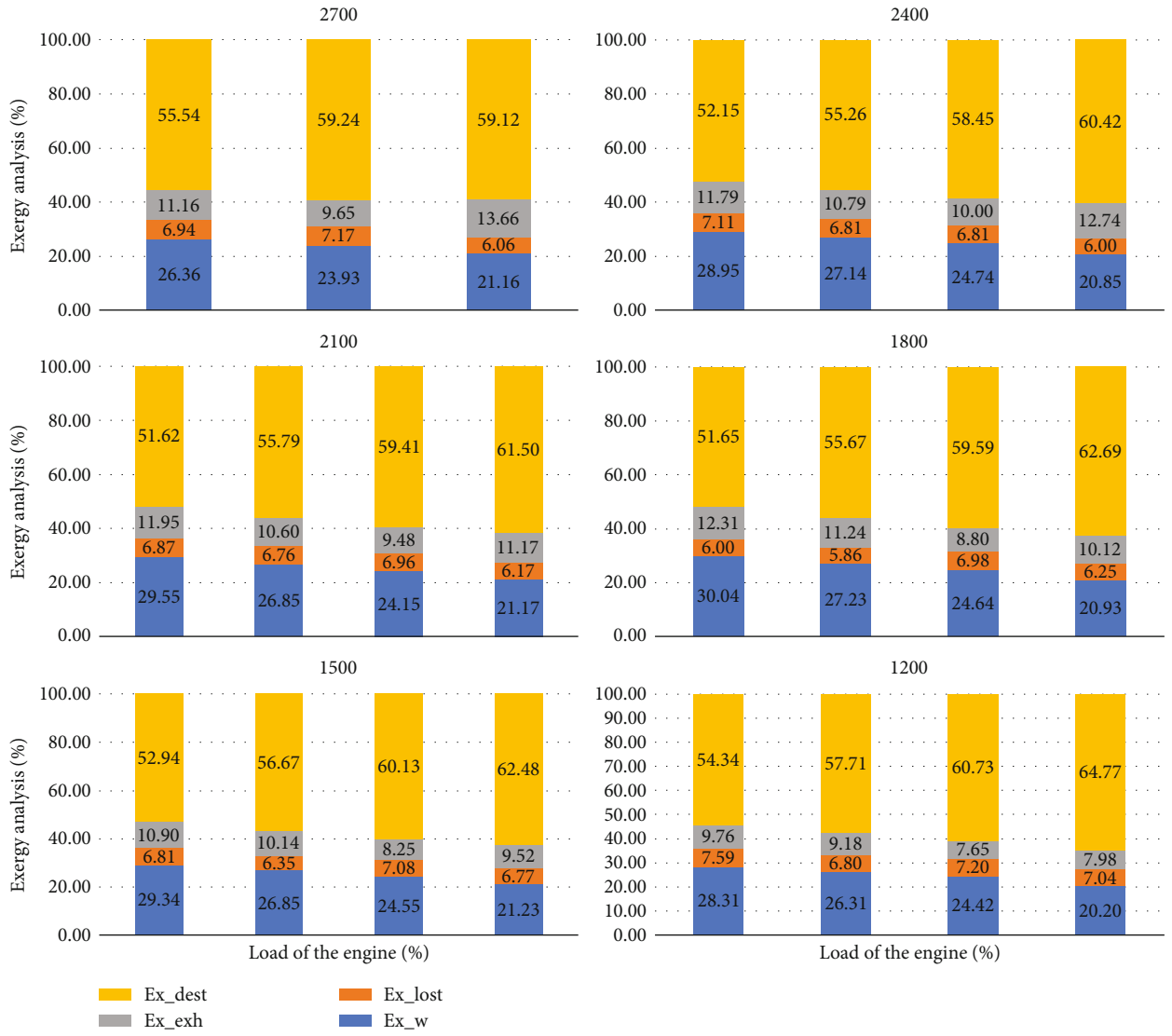

Figure 7: Results of exergy analysis of ammonia-fueled engine.

share of the cooling exergy (caused by a lower operating temperature). Described trends are generally true for the diesel and biodiesel variants as well; as such, the introduction of ammonia proves to be a feasible solution in terms of engine operation.

The comparison in terms of the ammonia-fueled variant to the diesel and biodiesel leads to the following observations. Firstly, introduction of ammonia to the engine changes the characteristic of efficiency; i.e., peak efficiency, throughout a set of the tested shaft's speeds, occurs at 100% load, not at 71% which is the case for diesel and biodiesel variants. This is true at all shaft speeds which is caused primarily by a better combustion of ammonia at the highest load. It can be observed by analyzing Table 8 which shows that for the case of the 71% load, the exhaust gases contain a similar share of ammonia in the exhaust, even though the mass flow rate of ammonia is lower. This is further confirmed by Figure 5 which proves that higher exergy destruction occurs at 71% compared to the 100% load. Still, in terms of the direct comparison of the efficiencies between these three type of fuels, it is seen that the ammonia-fueled variant achieves lower values in most cases, comparing the corresponding points. Secondly, further comparison of an ammonia-fueled variant to diesel reveals a lower exhaust energy than for the diesel case. This could be explained by a lower temperature of the exhaust gases for the ammonia-fueled variant and by values of the mass flow rates of the exhaust, compared to diesel at corresponding points. However, since the thermal efficiency is, for almost all cases, also lower, it implies the higher share of cooling losses, as seen when comparing Figures 2 and 6 (cooling losses are calculated by closing the energy balance, as explained in equation ((2))). The same relationship applies to the comparison of Figures 4–6 since the diesel and biodiesel cases represent very similar trends.

A comparison between the results of exergy assessments show that, for almost all cases independently of the shaft's speed or load, the exergy destruction has a higher share for ammonia than for diesel or biodiesel cases, roughly by 5 percentage points. It proves the need for engine optimization in

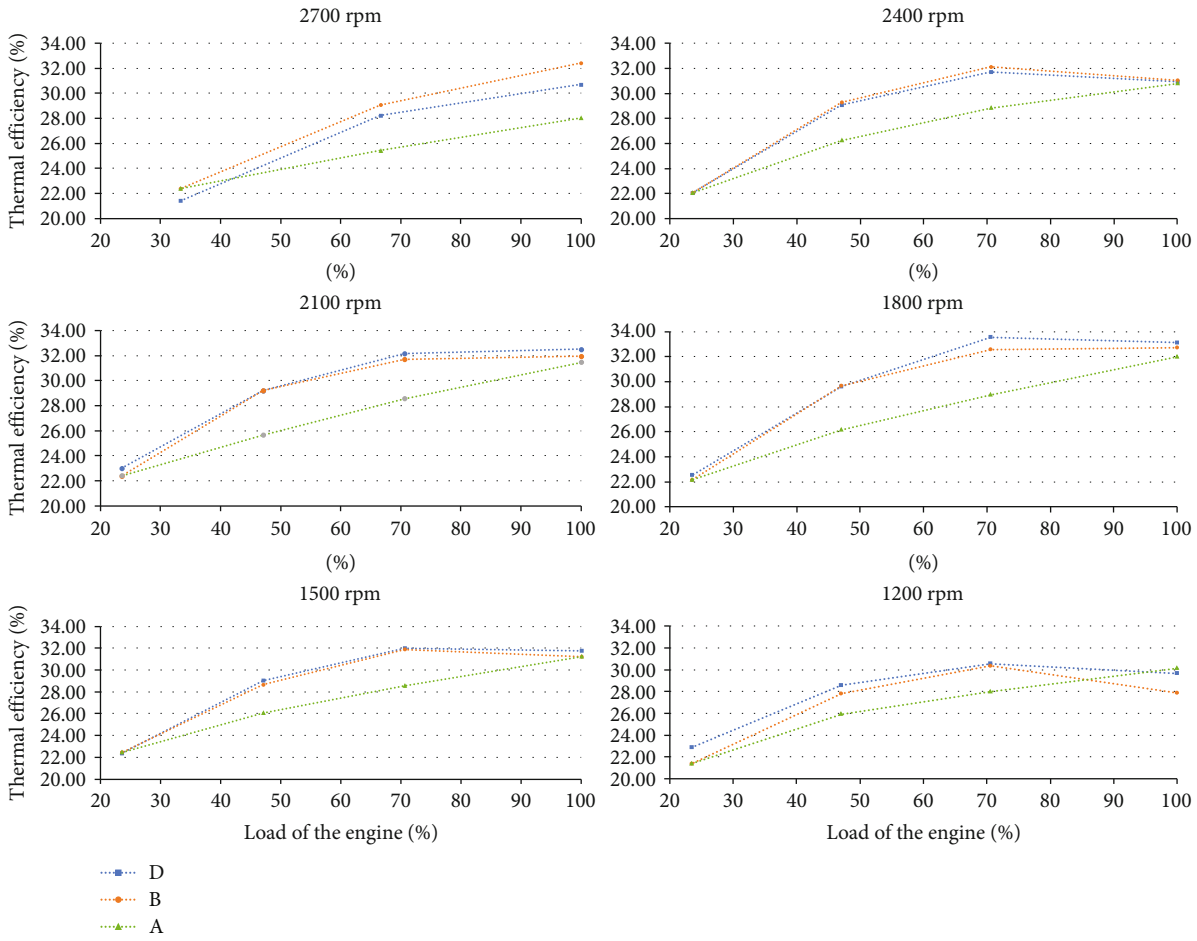

Figure 8: Thermal efficiency with respect to the engine's load and rpm.

terms of ammonia combustion. The share of exhaust exergy is higher for diesel and biodiesel cases compared to the ammonia-fueled engine which corresponds to the previously mentioned higher exhaust temperatures. A higher share of exergy lost to the environment (from the energy analysis) for the ammonia-fueled engine compared to diesel and biodiesel corresponds to the higher share of energy lost due to cooling.

The highest value of thermal efficiency across the engine's performance is achieved at 1800 rpm at 100% load with 31.98%; at the same point, the highest exergy efficiency is obtained to be 30.04%. An ideal waste heat recovery could theoretically increase this efficiency to 42.35%.

4.4. Fuel System Comparison. The results of particular analyses performed on the three types of fuel systems have been elaborated in the previous Sections 4.1, 4.2, and 4.3. Averaging the values over the engine's range (for a whole set of rpm as well as the load), the ammonia introduced to the engine, via port injection, impacts the energy balance of the engine in the following way (compared to diesel and biodiesel variants):

(1) Thermal efficiency is decreased

(2) Exhaust energy is decreased

(3) Heat lost due to cooling is increased

Exergy analysis leads to the following conclusions:

(1) Exergy efficiency and exergy of exhaust are decreased

(2) Exergy destruction and exergy of energy lost the environment are increased

Among these parameters, the thermal efficiency of the engine could be treated as the major criterion of the engine's performance. In order to understand the effect of introducing ammonia to this efficiency in a better way, Figure 8 has been plotted. It presents the thermal efficiency as a function of load with respect to a particular shaft's speed. A common trend for the efficiency of the diesel engine is that it achieves its peak value in between the engine operating range, as presented, e.g., by [23]. In the case of this study, it is generally seen that the engine is suited to perform more efficiently at high loads which correspond to the fact that the engine has been designed and tuned for the minitractor; such vehicles are designed to sustain high-load operation since they can be coupled with external devices and perform activities like mowing, spraying, sweeping, etc. Analyzing the diesel fuel trend, it is seen that a peak in between the engine's range

(71% load) is visible for 2400, 1800, 1500, and 1200 rpm; in the case of the 2700 and 2100 rpm, the highest value of thermal efficiency is at the 100% load. Low efficiency is noted at the lowest load of 24% for all shaft speeds. The results of thermal efficiency for the biodiesel-fueled engine indicate a similar trend. However, this behavior does not reflect the ammonia-fueled engine precisely, as, for this case, the peak occurs at the highest load for all speeds, and the relationship between the efficiency and the load is more linear. This could potentially indicate that even higher efficiencies might be achieved at higher loads, provided they fall within the engine's operating range (which could be verified on a larger-sized engine since the engine used in this study has been analyzed in terms of its whole range).

Independently of the load, at the highest rpm of 2700 and 2400, the peak efficiency is achieved by biodiesel. For 2100, 1800, 1500, and 1200 rpm, it is achieved by the diesel case, although, for this rpm, the ammonia-fueled variant achieves a very similar value (at 100% load; 0.2 percentage point difference). For most of the shaft's speeds, the differences between the three fuel systems at 24% and 100% are rather small. An apparent difference is seen for the 100% load at 2700 rpm, where the biodiesel-fueled engine achieved the higher efficiency by more than four percentage points compared to the ammonia-fueled variant. However, at medium loads, there is a difference of approximately two to three percentage points between the ammonia-fueled engine and the pure diesel and biodiesel cases. It shows the need for engine optimization in terms of adjusting the ammonia-pilot fuel ratio and optimizing the injection timing. If the engine was to be operated in a configuration that introduced ammonia, in order to minimize the thermodynamic losses, it should be operated at high loads. However, considering that the purpose of the engine is actually to perform activities designed for a minitractor, thus operating at high loads, ammonia introduction via port injection at default settings of the pilot fuel could be a feasible solution from the thermodynamic point of view.

The discussion presented so far is aimed at assessing the performance of the engine throughout its whole range, considering three types of fuel systems. However, as seen in Figure 8, for some points, the differences in the calculated results are very small. This is seen, for instance, at 2100 rpm and 100% load, where the thermal efficiency equals to 32.51%, 31.96%, and 31.45% for diesel, biodiesel, and ammonia scenarios, respectively. The underlying assumption behind the experimental research is the validity of the experiment data. The data provided are characterized by their uncertainty, as mentioned in Section 2; still, calculating the parameters such as the thermal efficiency based on these values are also characterized by an uncertainty which can be calculated using the uncertainty propagation method. Recalling equation (9) for the thermal efficiency, and equation (6) for the fuel energy rate, it is seen that the efficiency uncertainty depends on the measured value of the power of the engine, and the measured mass flow rate of fuel. The lower heating value of the respective fuel is also associated with an uncertainty; however, in order to simplify the calculations, it is going to be considered as a constant value. Under such an assumption, considering the partial derivatives of the thermal efficiency, the equation for the uncertainty of the thermal efficiency could be expressed as

Table 10: Efficiency and uncertainty comparison for three selected fueling systems for 2100 rpm and 100% load.

	Diesel	Biodiesel	Ammonia
η	32.509	31.962	31.454
$\delta\eta$	0.045	0.032	0.054

$$\delta\eta = \sqrt{\left(\frac{d\eta}{d\dot{W}}\delta\dot{W}\right)^2 + \left(\frac{d\eta}{d\dot{E}_{\text{fuel}}}\delta\dot{E}_{\text{fuel}}\right)^2}, \tag{20}$$

where $\delta\eta$ is the calculated uncertainty of the thermal efficiency, $\delta\dot{W}$ represents the uncertainty of the power of the engine, and $\delta\dot{E}_{\text{fuel}}$ stands for the uncertainty of fuel energy rate, calculated from the uncertainty propagation calculated for equation (6). The uncertainty of the fuel energy rate depends on the uncertainties of diesel, biodiesel, and ammonia mass flow rates.

Applying equation (20) on the example of 2100 rpm and 100% load, the results presented in Table 10 are obtained. It can be observed that the uncertainty associated with the calculated efficiency is small, which is a result of low uncertainties of the measured power and mass flow rates. This small uncertainty is primarily due to these values being derived from a set of measurements taken during the engine's steady-state operation, as explained in Section 2. While this process of uncertainty propagation could be repeated for other data points and calculated parameters, the resulting values are likely to be similarly small, given the observed trends. As such, the case study presented here is considered to provide sufficient understanding of these trends, and no further examination is carried out.

Results of the energy and exergy analyses for the diesel and biodiesel scenarios confirm the literature findings. Thermal and exergy efficiencies are similar to the values reported by the literature (close to 30-35%). Energy analysis indicates that about 65-70% of energy contained in the fuel is not effectively utilized, and the exergy balance proves the combustion and friction processes to account for most of the exergy destruction, e.g., [21, 24–26] (roughly around 50%).

From the thermodynamic point of view, ammonia seems to be a feasible solution; however, there are other crucial factors to consider prior to making ultimate conclusions regarding this technology. The first one would be to analyze the ammonia slip. For instance, as can be seen in Tables 7 and 8, at 2100 rpm and 71% load, the ammonia share in the exhaust is 1.627% at 6.9% oxygen level. This value is considered high given the toxic nature of ammonia. The second consideration should apply to NOx emissions. In this research, the NOx emissions have been excluded from the assessment since their impact on the energy and exergy balances is negligible. However, it is worth mentioning that even though NOx emissions are not critical for these specific assessments, they could have environmental implications,

especially in terms of the N_2O emission which is a greenhouse gas. Considering that the primary reason behind implementing an ammonia-fueled engine is to reduce the impact of the vehicle on climate change, high emissions of N_2O might offset the benefits of reducing carbon dioxide and methane. Even though a thorough investigation of the environmental impact of the ammonia-driven vehicle is outside the scope of this work, it could be a limiting factor towards widespread adoption of this technology.

5. Conclusions

In this work, a small-unit compression ignition (CI) engine is examined through energy and exergy assessments. These assessments are based on experimental data collected over the entire range of the engine, considering three fuel supply scenarios: diesel, biodiesel, and ammonia used in combination with biodiesel pilot oil. The ammonia was introduced to the engine using a port injection strategy. When considering the entire range of the engine, the maximum thermal efficiency of 33.56% and exergy efficiency of 31.88% were observed at 1800 rpm and 71% load for the diesel fuel system. For the biodiesel-fueled engine, thermal and exergy efficiencies of 32.72% and 30.93%, respectively, were achieved at 1800 rpm and full load. Lastly, the ammonia-fueled engine demonstrated thermal and exergy efficiencies of 31.98% and 30.04%, respectively, at 1800 rpm and full load. On average, the efficiency for the ammonia-fueled engine is slightly lower than in the case of diesel and biodiesel; however, this difference declines at maximum load (as in Figure 8), which is the trend observed for almost all of the shaft's speeds (apart from the highest 2700 rpm). For all three cases, the exergy destruction is responsible for the highest useful energy loss, and its optimization would bring the most improvement to the engine's performance.

A major advantage of utilizing ammonia in the internal combustion engine comes from the fact that it allows for the reduction of greenhouse gases such as CO_2 and CH_4. Still, further investigation towards the NH_3 slip and NOx emissions should be analyzed. One option would be to continue the development of the port injection system focusing on the optimization in terms of the ammonia-to-pilot fuel ratio, injection timing, or exhaust gas recirculation. Alternatively, a direct injection of ammonia could be a promising solution, especially towards solving the issue of NH_3 slip, as it would be aimed at improving the combustion. Direct injection could potentially improve the results of exergy assessment, since the ammonia-fueled scenario is characterized by a higher exergy destruction compared to the diesel and biodiesel cases.

To recapitulate, the work shows that from the thermodynamic point of view, ammonia can be a successful substitute of diesel and biodiesel oils for the compression ignition engine which is optimized to sustain heavy-load conditions, such as the analyzed engine, originally designed for a minitractor. However, the engine's optimization in terms its performance is required prior to the widespread popularisation of the technology.

Data Availability

Major data pertaining to this study are included. Supplementary data are available upon request.

Conflicts of Interest

The authors declare that they have no conflicts of interest.

Acknowledgments

The research leading to these results has received funding from the Norway Grants 2014-2021 under the POL-NOR2019 competition operated by the National Centre for Research and Development and from the Polish State Budget. The grant number is NOR/POLNOR/ACTIVATE/0046/2019-00.

References

[1] A. Aljaafari, I. M. R. Fattah, M. I. Jahirul et al., "Biodiesel emissions: a state-of-the-art review on health and environmental impacts," *Energies*, vol. 15, no. 18, p. 6854, 2022.

[2] US Energy Information Administration, "Biofuels explained - biofuels and the environment," 2022, https://www.eia.gov/energyexplained/biofuels/biofuels-and-the-environment.php.

[3] European Federation for Transport and Environment, "Biofuels twice as expensive as petrol and diesel in most cases," 2022, https://www.transportenvironment.org/discover/biofuels-are-twice-as-expensive-as-fossil-fuels/.

[4] L. Jakub, "Ammonia and conventional engine fuels: comparative environmental impact assessment," *E3S Web of Conferences*, vol. 44, article 00091, 2018.

[5] C. Mounaim-Rousselle and P. Brequigny, "Ammonia as fuel for low-carbon spark-ignition engines of tomorrow's passenger cars," *Frontiers in Mechanical Engineering*, vol. 6, p. 70, 2020.

[6] Y. A. Cengel and M. A. Boles, *Thermodynamics: An Engineering Approach*, McGraw-Hill College, Boston, MA, USA, 2006.

[7] N. Damanik, H. C. Ong, C. W. Tong, T. M. I. Mahlia, and A. S. Silitonga, "A review on the engine performance and exhaust emission characteristics of diesel engines fueled with biodiesel blends," *Environmental Science and Pollution Research*, vol. 25, no. 16, pp. 15307–15325, 2018.

[8] M. Abedin, H. Masjuki, M. Kalam, A. Sanjid, S. A. Rahman, and B. Masum, "Energy balance of internal combustion engines using alternative fuels," *Renewable and Sustainable Energy Reviews*, vol. 26, pp. 20–33, 2013.

[9] M. Abedin, A. Imran, H. Masjuki et al., "An overview on comparative engine performance and emission characteristics of different techniques involved in diesel engine as dual-fuel engine operation," *Renewable and Sustainable Energy Reviews*, vol. 60, pp. 306–316, 2016.

[10] M. Abdelrazek, M. Abdelaal, and A. El-Nahas, "Numerical simulation of a diesel engine performance powered by soybean biodiesel and diesel fuels," *Beni-Suef University Journal of Basic and Applied Sciences*, vol. 12, no. 1, 2023.

[11] B. Karpanai Selvan, S. Das, M. Chandrasekar et al., "Utilization of biodiesel blended fuel in a diesel engine - combustion engine performance and emission characteristics study," *Fuel*, vol. 311, article 122621, 2022.

[12] S. Thiyagarajan, E. Varuvel, V. Karthickeyan et al., "Effect of hydrogen on compression-ignition (CI) engine fueled with vegetable oil/biodiesel from various feedstocks: a review," *International Journal of Hydrogen Energy*, vol. 47, no. 88, pp. 37648–37667, 2022.

[13] O. H. Ghazal, "Performance and combustion characteristic of CI engine fueled with hydrogen enriched diesel," *International Journal of Hydrogen Energy*, vol. 38, no. 35, pp. 15469–15476, 2013.

[14] S. Jafarmadar, "Exergy analysis of hydrogen/diesel combustion in a dual fuel engine using three-dimensional model," *International Journal of Hydrogen Energy*, vol. 39, no. 17, pp. 9505–9514, 2014.

[15] H. Taghavifar, S. Khalilarya, S. Mirhasani, and S. Jafarmadar, "Numerical energetic and exergetic analysis of CI diesel engine performance for different fuels of hydrogen, dimethyl ether, and diesel under various engine speeds," *International Journal of Hydrogen Energy*, vol. 39, no. 17, pp. 9515–9526, 2014.

[16] E. Nadimi, G. Przybyla, D. Emberson, T. Lovas, L. Ziolkowski, and W. Adamczyk, "Effects of using ammonia as a primary fuel on engine performance and emissions in an ammonia/biodiesel dual-fuel CI engine," *International Journal of Energy Research*, vol. 46, no. 11, pp. 15347–15361, 2022.

[17] E. Nadimi, G. Przybyła, M. T. Lewandowski, and W. Adamczyk, "Effects of ammonia on combustion, emissions, and performance of the ammonia/diesel dual-fuel compression ignition engine," *Journal of the Energy Institute*, vol. 107, article 101158, 2023.

[18] K. Kuta, G. Przybyła, D. Kurzydym, and Z. Żmudka, "Experimental and numerical investigation of dual-fuel CI ammonia engine emissions and after-treatment with V_2O_5/SiO_2-TiO_2 SCR," *Fuel*, vol. 334, article 126523, 2023.

[19] Z. Zhang, W. Long, P. Dong et al., "Performance characteristics of a two-stroke low speed engine applying ammonia/diesel dual direct injection strategy," *Fuel*, vol. 332, article 126086, 2023.

[20] N. Al-Najem and J. Diab, "Energy-exergy analysis of a diesel engine," *Heat Recovery Systems and CHP*, vol. 12, no. 6, pp. 525–529, 1992.

[21] B. G. Şanli and E. Uludamar, "Energy and exergy analysis of a diesel engine fuelled with diesel and biodiesel fuels at various engine speeds," *Energy Sources, Part A: Recovery, Utilization, and Environmental Effects*, vol. 42, no. 11, pp. 1299–1313, 2020.

[22] A. Çakmak and A. Bilgin, "Exergy and energy analysis with economic aspects of a diesel engine running on biodiesel-diesel fuel blends," *International Journal of Exergy*, vol. 24, no. 1/2, p. 1, 2017.

[23] R. Karami, M. Hoseinpour, M. Rasul, N. Hassan, and M. Khan, "Exergy, energy, and emissions analyses of binary and ternary blends of seed waste biodiesel of tomato, papaya, and apricot in a diesel engine," *Energy Conversion andManagement: X*, vol. 16, article 100288, 2022.

[24] B. S. Kul and A. Kahraman, "Energy and exergy analyses of a diesel engine fuelled with biodiesel-diesel blends containing 5% bioethanol," *Entropy*, vol. 18, p. 387, 2016.

[25] I. Nazzal and R. Al-Doury, "Exergy and energy analysis of diesel engine fuelled with diesel and diesel-corn oil blends," *Journal of Advanced Research in Fluid Mechanics and Thermal Sciences*, vol. 63, pp. 92–106, 2019.

[26] G. Khoobbakht, A. Akram, M. Karimi, and G. Najafi, "Exergy and energy analysis of combustion of blended levels of biodiesel, ethanol and diesel fuel in a DI diesel engine," *Applied Thermal Engineering*, vol. 99, pp. 720–729, 2016.

[27] M. Hoseinpour, H. Sadrnia, M. Tabasizadeh, and B. Ghobadian, "Energy and exergy analyses of a diesel engine fueled with diesel, biodiesel-diesel blend and gasoline fumigation," *Energy*, vol. 141, pp. 2408–2420, 2017.

[28] X. Wang, B. G. Sun, and Q. H. Luo, "Energy and exergy analysis of a turbocharged hydrogen internal combustion engine," *International Journal of Hydrogen Energy*, vol. 44, no. 11, pp. 5551–5563, 2019.

[29] X. Yu, D. Li, P. Sun, G. Li, S. Yang, and C. Yao, "Energy and exergy analysis of a combined injection engine using gasoline port injection coupled with gasoline or hydrogen direct injection under lean-burn conditions," *International Journal of Hydrogen Energy*, vol. 46, no. 11, pp. 8253–8268, 2021.

[30] P. Sun, Z. Liu, X. Yu, C. Yao, Z. Guo, and S. Yang, "Experimental study on heat and exergy balance of a dual-fuel combined injection engine with hydrogen and gasoline," *International Journal of Hydrogen Energy*, vol. 44, no. 39, pp. 22301–22315, 2019.

[31] A. O. Hasan, A. I. Osman, A. H. Al-Muhtaseb et al., "An experimental study of engine characteristics and tailpipe emissions from modern DI diesel engine fuelled with methanol/diesel blends," *Fuel Processing Technology*, vol. 220, article 106901, 2021.

[32] C. Michalakakis, J. Fouillou, R. Lupton, A. Gonzalez Hernandez, and J. Cullen, "Calculating the chemical exergy of materials," *Journal of Industrial Ecology*, vol. 25, no. 2, pp. 274–287, 2021.

[33] J. Szargut, *Exergy Method: Technical and Ecological Applications*, WIT Press, 2006.

[34] J. Szargut, *Egzergia, Poradnik Obliczania i Stosowania*, Wydawnictwo Politechniki Slaskej, 2007.

[35] Y. J. Ramos da Costa, A. G. Barbosa de Lima, C. R. Bezerra Filho, and L. de Araujo Lima, "Energetic and exergetic analyses of a dual-fuel diesel engine," *Renewable and Sustainable Energy Reviews*, vol. 16, no. 7, pp. 4651–4660, 2012.

[36] A. Nair and F. Yu, "Quantification of atmospheric ammonia concentrations: a review of its measurement and modeling," *Atmosphere*, vol. 11, no. 10, p. 1092, 2020.

[37] Engineering Tool Box, "Air - molecular weight and composition," 2004, https://www.engineeringtoolbox.com/molecular-mass-air-d_679.html.